NASA TECHNICAL MEMORANDUM NASA TM-75655

ON THE POSSIBILITY OF ANALYTICAL APPROXIMATION OF LINE FORMS DURING RANDOM DISORDERS OF THE RESONANCE FREQUENCIES IN MOLECULAR VIBRATION-ROTATION SPECTRA FOR SATELLITE SOUNDING

V. V. Fomin

Translation of "O vozmozhnosti analiticheskoy approksimatsii formy liniy pri proizvol'nykh rasstroykakh rezonansnykh chastot v kolebatel'no-vrashchatel'nykh spektrakh molekul dlya tseley sputnikovogo zondirovaniya," Institute of the Optics of the Atmosphere, Siberian Section, USSR Academy of Sciences, Tomsk, Report, 1978, pp. 1-67

NATIONAL AERONAUTICS AND SPACE ADMINISTRATION
WASHINGTON, D.C. 20546 JULY 1979

STANDARD TITLE PAGE

1. Report No. NASA TM-75655	2. Government Accession No.	3. Recipient's Catalog No.
4. Title and Subtitle ON THE POSSIBILITY OF ANALYTICAL APPROXIMATION OF LINE FORMS DURING RANDOM DISORDERS OF THE RESONANCE FREQUENCIES IN MOLECULAR VIBRATION-.....		5. Report Date July 1979 6. Performing Organization Code
7. Author(s) V.V. Fomin, Inst. of Optics of the Atmosphere, Siberian Sec. USSR Acad. of Sciences, Tomsk		8. Performing Organization Report No. 10. Work Unit No.
9. Performing Organization Name and Address Leo Kanner Associates Redwood City, California 94063		11. Contract or Grant No. NASw-3199 13. Type of Report and Period Covered Translation
12. Sponsoring Agency Name and Address National Aeronautics and Space Administration, Washington, D.C. 20546		14. Sponsoring Agency Code

15. Supplementary Notes

Translation of "O vozmozhnosti analiticheskoy approksimatsii formy liniy pri proizvol'nykh rasstroykakh rezonancnykh chastot v kolebatel'no-vrashchatel'nykh spektrakh molekul dlya tseley sputnikovogo zondirovaniya," Institute of the Optics of the Atmosphere, Siberian Section, USSR Academy of Sciences Tomsk, Report, 1978, pp. 1-67

16. Abstract Available line contour approximations are surveyed. The generalized spectral line contour concept and formulas for a two component mixture, as well as consequences of the general formula are discussed. The calculation procedure, initial information, calculation results and comparison of calculations with available experimental data, for radiation absorption in 3 CO_2 bands are presented. Further research on the temperature dependence of the absorption coefficient, problems of increasing accuracy and further verification of the efficiency of the approach developed are proposed.

17. Key Words (Selected by Author(s))	18. Distribution Statement
	Unclassified-Unlimited

19. Security Classif. (of this report)	20. Security Classif. (of this page)	21. No. of Pages	22. Price
Unclassified	Unclassified	71	

Item XIX of list of works to be performed by USSR, in accordance with program of coordinated Soviet-American studies to improve methods of satellite atmospheric temperature sounding; Appendix III to protocol of third meeting of Soviet-American working group on space meteorology, Moscow, USSR, 10-22 November 1976.

TABLE OF CONTENTS

ON THE POSSIBILITY OF ANALYTICAL APPROXIMATION OF LINE FORMS DURING RANDOM DISORDERS OF THE RESONANCE FREQUENCIES IN MOLECULAR VIBRATION-ROTATION SPECTRA FOR SATELLITE SOUNDING

V. V. Fomin
Academy of Sciences USSR, Siberian Department,
Institute of the Optics of the Atmosphere, Tomsk

Introduction

The paper presents some results of investigations carried /3* out at the statistical optics laboratory, Institute of Atmosphereic Optics, Siberian Branch, USSR Academy of Sciences, within the framework of "Program of Coordinated American-Soviet Studies to Improve Methods of Satellite Atmospheric Temperature Sounding" in accordance with Section III, "Agreement on a General Catalog of the Fine Structure Parameters of the Atmospheric Gases from the Results of Laboratory and Theoretical Studies."

Concerning the accuracy of assignment of the initial spectroscopic information in the satellite sounding problem, two significant features can be pointed out: 1. the lack of valid expressions which reflect the physical regularities of absorption on the periphery of spectral lines and bands, which enable consistent description of current experimental data; 2. the corresponding unpredictability of errors of the absorption coefficients at smaller intermediate values of the shifted frequencies. Besides these significant errors connected with the frequency dependence of the absorption coefficient, the fundamental nature of these features for satellite problems is increased, because they prove to be intimately connected with the

---

* Numbers in the margin indicate pagination in the foreign text.

form of the functional dependence of the weighting functions on temperature and concenteration, i.e., on the characteristics which are the object of sounding.

The aim of our investigations was to determine the possibilities of constructing a theory of radiation absorption in the wings of vibration-rotation bands allowed by the selection rules, with the finite goal of obtaining analytical expressions, which could be used to calculate weighting functions.

Analysis showed that, in contrast to the central portion of /4 a line, for which current methods of analysis of different authors actually are similar to the system of kinetic equations in the resonance approximation (the latter determines the upper limit of frequency shifts), for the periphery of a line, the asymptotic approach is highly efficient. It permits estimation of the time integrals, features of the problem connected with its quantum nature, to be reduced to analysis of the equations for stationary points, statistical interpretation of the classical dynamic collision processes to be given and, finally, the result to be obtained in the form of visible, analysable formulas. A systematic discussion of the theory is given in monograph [1], where the efficiency of the theory has been verified, using extensive experimental material, including various molecules, gaseous mixtures, spectral ranges and absorption and emission spectra.

A theoretical analysis also successfully showed that the same intermolecular distances, interactions at which effectively appear as broadening, correspond to the regions of small and large frequency shifts at the common boundary ($t = 1$), though they are extreme opposite cases ($t \ll 1$ and $t \gg 1$, where $t \sim |\nu - \nu_0|$ is the shifted frequency). Furthermore, in some cases (for

example, self-broadening of polar molecules) on the common boundary, the corresponding spectral distributions of intensity correspond to these cases. These facts permitted approximation of the contour to be proposed in the intermediate region of shifted frequencies.

Thus, the principal result of the paper is the formulation of the possibility of introduction of a physically valid line contour, which permits calculation of the absorption coefficient (and, hence, the weighting function) at frequencies arbitrarily distant from the center of the line, i.e., the incorporation of a contour which describes the entire line. (Below, the term "generalized line contour" is used.) /5

The efficiency of the expression obtained was verified with limited experimental material, the results from [2-4], on radiation absorption on the peripheries of the high-frequency wings of the 4.3 μm, 2.7 μm and 1.4 μm carbon dioxide bands. The cases of self-broadening and broadening by molecular nitrogen were investigated. Numerical calculations permit illustration of the possibility of the use of simplified formulas with a small number of parameters. As the next stage, the paper suggests the conduct of special experiments in additional, comprehensive verification of the validity of the expression, the accuracy of the absorption coefficient values obtained with it and, also, correlation of the contour obtained with specific sounding channels.

In Section I, a summary of the formulas commonly used for calculation of absorption coefficients in atmospheric applications is presented. Approximate expressions suggested by various authors are presented, and the ambiguity and inconsistency of the results are stated, based on analysis of the empirical data.

In Section II, the "generalized line contour" is introduced. The basic features which indicate the physical essence of the expressions obtained and some of their consequences are noted.

In Section III, the procedure for calculations is presented, based on the proposed expression for the line form. The results of numerical calculations for the carbon dioxide spectrum are discussed. A comparison with experimental data is made.

In final Section IV, some consequences of the discussion are summarized, and proposals for the conduct of experiments and further theoretical studies of this question are formulated.

Figures and tables are presented in Appendices. All the figures reproduce the data of the tables.

G. V. Telegin, a scientific associate of the statistical optics laboratory, participated in the investigations and preparation of the report.

1. Brief Discussion of Available Line Contour Approximations

It can be considered well demonstrated that, under actual /6 atmospheric conditions, the basic causes of spectral line broadening are collision relaxation and the velocity distribution of particles. The first mechanism is prevalent over a considerable spectral interval in the troposphere and lower stratosphere. And what is more, with increase in resonance frequency disorders, the effectiveness of Doppler broadening decreases exponentially (a more detailed discussion of this question can be found in monographs [5,6]). Because of this, all the emphasis in the paper is placed on the collision broadening mechanism.

Further, information is presented on the spectral dependence of the absorption coefficient. In this case, the goal is not to give a detailed survey of existing work but only current approximations and some available experimental facts are considered.

Theory gives the following formulas for calculation of absorption coefficient $k(\nu)$ at frequency ν:

Lorentz (dispersion) contour [7]

$$k(\nu) \equiv k_L(\nu) = \frac{S}{\pi} \frac{\gamma}{(\nu-\nu_0)^2+\gamma^2} \tag{1}$$

Complete Lorentz contour [8]

$$k(\nu) \equiv k_{FL}(\nu) = \frac{S}{\pi} \left(\frac{\nu}{\nu_0}\right) \left[\frac{\gamma}{(\nu-\nu_0)^2+\gamma^2} - \frac{\gamma}{(\nu+\nu_0)^2+\gamma^2}\right] \tag{2}$$

Van Vleck-Weisskopf contour [9]

$$k(\nu) \equiv k_{VVW}(\nu) = \frac{S}{\pi} \left(\frac{\nu}{\nu_0}\right)^2 \left[\frac{\gamma}{(\nu-\nu_0)^2+\gamma^2} + \frac{\gamma}{(\nu+\nu_0)^2+\gamma^2}\right] \tag{3}$$

As was shown in [1], current discussion [9x] of the utilization of formulas (2) and (3) are underway on the correct calculation of expressions for the integral line intensity. /7

Kinetic equation contour [10]

$$k(\nu) \equiv k_K(\nu) = \frac{S}{\pi} \frac{4\nu^2\gamma}{(\nu_0^2-\nu^2)^2+4\nu^2\gamma^2} . \quad (4)$$

In expressions (1) - (4) and below, ν_0, S and γ are the position of the line center, its integral intensity and its half width.

Theory predicts possible deviations of the frequency dependence from (1) - (4) (see, for example, survey [11]). As applied to atmospheric problems, the mechanism of interference effects [12,13] for groups of lines located close together (for example, the Q branches) deserves attention. However, for actual atmospheric conditions, it still has not been confirmed.

Formulas (1) - (4) were obtained on the common assumption of the "instantaneous nature" of molecular interactions. The methods of obtaining them can be translated into the language of kinetic equations in the resonance approximation (see, for example, [14]), in which the "instantaneous" condition and the resonance approximation are similar to each other and place an "upper" limit on the region of applicability of formulas (1) - (4)

$$\Delta\nu = |\nu-\nu_0| < \Delta\nu_0 \quad (5)$$

In the region of the infrared spectrum of interest to us ($\nu_0 > \gamma$), the fact that the absorption coefficients calculated over contours (1) - (4) have practically coincident values in small disorders of the resonance frequencies takes this into account. With increase in ν_0, this tendency is strengthened still more. As an illustration, values of the line form factor $f(\nu - \nu_0) = k(\nu)/S$, calculated by formulas (1) - (4) for two hypothetical lines, with parameters close to the parameters of the molecular nitrogen broadened water vapor lines, are given in Fig. 1 and Fig. 2 (see also Tables 1,2). In connection with this, the utilization of the rather simple Lorentz contour [5, 15] in the numerous calculations connected with atmospheric optics problems is completely justified. /8

On the other hand, the formal use of formulas (1) - (4), i.e., disregard of conditions (5), brings out significant discrepencies on the line peripheries. This is seen particularly well in the limiting transitions

$$|\nu - \nu_0| \gg \gamma \quad (\nu_0 \gg \gamma)$$

$$\left\{ \begin{array}{ll} \nu \to 0: & k_L(\nu) \to \frac{S}{\pi} \frac{\gamma}{\nu_0^2}; \\ & k_{FL}(\nu) = k_K(\nu) \to \frac{S}{\pi} \frac{4\nu^2\gamma}{\nu_0^4}; \\ & k_{VVW}(\nu) \to \frac{S}{\pi} \frac{2\nu^2\gamma}{\nu_0^4}; \end{array} \right. \qquad (6a)$$

$$\left\{ \begin{array}{ll} \nu \to \infty: & k_L(\nu) \to \frac{S}{\pi} \frac{\gamma}{\nu^2}; \\ & k_{FL}(\nu) = k_K(\nu) \to \frac{S}{\pi} \frac{4\gamma}{\nu^2}; \\ & k_{VVW}(\nu) \to \frac{S}{\pi} \frac{2\gamma}{\nu_0^2}. \end{array} \right. \qquad (6b)$$

The graphs presented in Figs. 1, 2 also graphically display the current discrepencies in the absorption coefficients, in the use of contours (1) - (4) with large frequency shifts.

It follows from the information presented that there are no arguments for the use of a given contour in calculations of transmission in the "transparency windows" of the actual atmosphere. In connection with this, we note the failure of attempts to describe the experimental results in the 8-12 μm and 2-36 cm^{-1} atmospheric "transparency windows", by means of (1) - (4) [10,16, 17].

The statistical contour [18,19]: /9

$$k \equiv k_{st}(\nu) = \frac{S}{\pi} \frac{N}{4m} \frac{\delta^{3/m}}{(\nu-\nu_0)^{1+3/m}}, \quad (m \geqslant 3), \tag{7}$$

where N is the concentration of broadened particles and δ and m are parameters connected with the interaction potential model.

The reasoning which led to the statistical contour gives a "lower" limit on the region of its applicability, i. e., in distinction from formulas (1) - (4), it is valid only in the region of large frequency shifts (line periphery) [18]. This appears in the divergence of expression (7) as Δν approaches zero. Simple estimates show that the statistical theory which result in the elimination of this divergence and, correspondingly to expansion of the region of permissible values of Δν, are applicable at elevated pressures which do not occur in the atmosphere of the earth. The spectral course of the absorption coefficient in the statistical contour is functionally nearly disperse, although it is still less sharply marked:

$$\frac{k_L(\nu)}{k_{st}(\nu)} \sim \frac{\gamma}{\delta^{3/m}} \Delta\nu^{3/m-1}.$$

We consider some experimental studies, in which deviations from relationships (1) - (4) and (7) were recorded.

It was found in [20] that, in pure NO, in the intervals between the vibration-rotation lines of the 5.3 μm band, distribution (7) is valid with $\underline{m} = 1.6$. In [21, 22], at frequencies shifted on the order of 10 cm^{-1}, an excess also was found above the dispersion contour for NH_3-N_2 mixtures with $\underline{m} = 0.88$ (10 μm band). At the same time, analysis of the results of [23, 24] indicate that, at $\Delta\nu > 100$ cm^{-1}, the intensity distribution of this mixture is significantly lower than (1), (7) (discrepency by orders of magnitude, according to the estimates of [25]). Information in [26], on CO absorption in the 2220 cm^{-1} - 2260 cm^{-1} spectral region (self-broadening case), also indicates a non-Lorentz intensity distribution in which the values of $k(\nu)$ turn out to be less than by formula (1). In [27, 28], it was proposed to describe the empirical data by the following expression:

$$k(\nu) = \frac{S}{\pi} \frac{m}{2} \sin\frac{\pi}{m} \frac{\delta^{m-1}}{(\nu-\nu_0)^m + \delta^m}. \qquad (8)$$

For a NH_3-H_2 mixture, $\underline{m} = 1.75$; for a HCl-CO_2 mixture, $\underline{m} = 1.75$ in the 2950 cm^{-1} - 3000 cm^{-1} spectral range.

Studies of radiation absorption at the edge of the 4.3 μm CO_2 band in mixtures of various gases led the authors of [2] to

a modified Lorentz contour

$$k(\nu)=k_L(\nu)\exp\left\{-a|\nu-\nu_0-\nu_{min}|^b\right\};\quad |\nu-\nu_0|\geqslant\nu_{min}, \tag{9}$$

where a, b and ν_{min} are parameters determined from experimental data (see Section 3). The exponential drop in the 4.3 μm band was confirmed by the authors of [3,4,29]. In [3], a sharp drop in absorption also was found in the 2.7 μm and 1.4 μm band. In [29], expression (9) is modified somewhat by the introduction of a fourth adjustment parameter which, however, can be disregarded within 10% error. The 15 μm, 4.3 μm, 2.7 μm, 20 μm, 1.6 μm and 1.4 μm bands were investigated in [29], and the set of parameters for pure CO_2 and CO_2 mixed with N_2 is given for each of them.

Study of the 118 GHZ oxygen line resulted in the following line form [30]

$$k(\nu)=6.69\times10^{-4}\frac{\nu^2\gamma^{0.65}}{(\nu-\nu_0)^{1.65}+\gamma^{1.65}}. \tag{10}$$

Experiments on the self-broadening of CS_2 and C_6H_6 have shown that the intensity distribution is given by the formula [31] /11

$$k(\nu)=\frac{k_0}{1+[\tau_c/|\nu-\nu_0|]^2}\frac{\gamma^2}{4(\nu-\nu_0)^2+\gamma^2}+$$

$$+\frac{|\nu-\nu_0|^{1.5}}{\beta}\frac{\exp\{-|\nu-\nu_0|\alpha\}}{1-\exp\{-hc|\nu-\nu_0|/\kappa T\}}, \tag{11}$$

where k_0 is the intensity in the center of the band, and α, β and τ_c are the adjustment parameters. For CS_2, adjustment of the high frequency wing of the band gave: $\tau_c = 10^{-12}$ sec (1ps), α = 0.100 cm, β = 738 $cm^{1.5}k_0$ and γ = 3.88 cm^{-1}.

The necessity for modification of contour (4), for the interpretation of data in the transparency windows of the millimeter and submillimeter spectral range of water vapor is pointed out in [32]:

$$k(\nu) = \frac{S}{\pi} \frac{4\nu_0^{2-z}\nu^2\gamma}{(\nu^2-\nu_0^2)^2+4\gamma^2\nu^2\nu_0^{2-z}}, \quad z = 1.6 \tag{12}$$

We note in conclusion that, despite present indications of the limited nature of relationships (1) - (4), they are used very actively in calculations at random frequencies, in the expanding group of problems of atmospheric optics and spectroscopy [5, 15]. This particularly concerns Lorentz contour (1).

2. Generalized Spectral Line Contour /12

2.1. Contour Form for Two Component Mixture

A generalized line contour is the result of the formal joining of the contours for the limiting cases of large and small disorders of the resonance frequencies. Such a statement of the problem is not unambiguous. However, the difficulties of

mathematical derivation of an intermediate portion of a contour (and the more so for the entire line) and the impossibility of obtaining it in the form of elementary functions for known special functions are well known. The significance of the result obtained intthis approach evidently has to depend on correct accounting for the regularities of the effect of molecular interactions on spectral line broadening and the tendency of mutual transition of the limiting cases, namely: 1. the presence of the "multipole interaction spectral dispersion effect"; 2. coincidence of the collision parameters forming the lower boundary of the wing and the upper boundary of the central portion; 3. coincidence of the frequency dependence of the dispersion contour with the form of the periphery, in coincidence of a lower order multipole interaction with the resonance dipole.

We explain this. If correction $\Delta(R)$ for the shift of the resonance frequency ν_0 is represented in the form of a multipole series

$$\Delta(R)=\sum_m \frac{C_m}{R^m}, \qquad (13)$$

where R is the intermolecular distance, in contrast to the center of the line in calculations of the form of the periphery, the spectral dispersion effect will appear. Different multipoles will effect both the numerical values of the contour parameter, and the form of the frequency distribution. In considering the central portion of the line, it can be shown [18] that there are some effective values R, at which broadening occurs. These R /13 unambiguously determine parameter γ. In calculation of γ, the contributions of different multipoles are summed and, in this manner, the presence of various multipoles results only in refinement of the paremeter. In this case, the multipole with minimum m for a given gaseous mixture makes the basic contribution,

as a rule. The following relationship is valid for R [18]

$$R \sim (C_m/v)^{1/m-1} \tag{14}$$

where v is the relative velocity of the molecules.

According to [1, 33], the role of different multipoles on the line periphery changes, depending on the frequency region of the line center under consideration. The determining tendency is an increase of the contribution to the numerical value of the absorption coefficient by higher order multipoles with shift to the wing and a simultaneous decrease in the role of lower order multipoles. In the area of the lower boundary of the periphery, the multipole with minimum m is decisive. For the effective interaction distance in this region, it can be written that

$$\Delta\nu > \Delta\nu_{min} = \frac{v}{R}; \quad R \sim \left[\frac{C_m(\Delta\nu)}{\Delta\nu}\right]^{1/m}; \quad C_m(\Delta\nu) \approx C_m \tag{15}$$

By substituting the lower limit of permissible $\Delta\nu$ in (15), it is easy to determine that (15) changes to (14). That is, the two opposite limiting cases, large and small $\Delta\nu$, turn out to be joined at this point. Moreover, it is easy to see that, with m = 3 (case of self-broadening and interaction of polar molecules with resonance terms in the general system of energy levels), distribution (7) (see also (30)), which is a partial case of the more general treatment [1, 33], coincides to within a factor with dispersion (1). With the connection of different multipoles

taken into account in calculation of the effective distances R, a shift of $\Delta\nu$ is produced (see (23)). It is easy to reach an expression for the "generalized line contour," in the case of a two component mixture. /14

$$k(\nu)/S \equiv f(\nu-\nu_0) = \frac{1}{\pi}\frac{\gamma}{(\nu-\nu_0)^2+\gamma^2}\,\omega(\nu-\nu_0) \tag{16}$$

$$\omega(\nu-\nu_0) = \frac{1-\exp\{-h\nu/\kappa T\}}{1-\exp\{-h\nu_0/\kappa T\}}\,\frac{\nu}{\nu_0}\,\frac{\pi(\nu-\nu_0)^2}{\gamma}\left[\varkappa_f + \varkappa_s\right] \tag{17}$$

An additional term with the frequency sum

$$\left[\exp\{-h\nu_0/\kappa T\}\,\omega(\nu+\nu_0)\right] \tag{18}$$

must be taken into account in expression (16), if the formula is used for lines in the far infrared region; $f(\nu-\nu_0)$ is the line form factor; subscripts s and f set apart the terms for self-broadening and broadening by the extraneous gas; $\gamma = \gamma_s + \gamma_f$ and γ_s and γ_f are the partial half widths. The formulas for the other quantities are:

$$\varkappa_{f,s} = K_{f,s}(\nu-\nu_0)\,\varphi(R_{f,s}) \tag{19}$$

$$K_{f,s}(\nu-\nu_0) = \frac{4\pi N_{f,s} R_{f,s}^3}{\sum\limits_{l=3,m,\kappa} l\, C_l^{(f,s)}/R_{f,s}^l} \tag{20}$$

$$\varphi(R_{f,s}) = \frac{1}{R_{f,s}} \int_0^{R_{f,s}} \frac{R \exp\{-U(R)/kT\}}{\sqrt{R_{f,s}^2 - R^2}} dR \qquad (21)$$

$$R_{f,s} = \left\{ \left(C_3^{(f,s)} + \sqrt{C_3^{(f,s)2} + 4\Delta\nu^{2\frac{m-3}{m}} C_m^{(f,s)\frac{6}{m}}(\Delta\nu)} \right) / 2\Delta\nu \right\}^{1/3}; \qquad (22)$$

$$C_m^{(f,s)}(\Delta\nu) = \left(C_m^{(f,s)} + \sqrt{C_m^{(f,s)2} + 4\Delta\nu^{2\frac{k-m}{k}} C_k^{(f,s)\frac{2m}{k}}(\Delta\nu)} \right) / 2; \qquad (23)$$

$$C_3^{(f,s)} = 3\gamma_{f,s} / 4\pi^2 N_{f,s}. \qquad (24)$$

In (20) - (24) N_I is the particle concentration of the corresponding component; $C_\ell^{(f,s)}$ is included in expression (13) (with the exception of $\ell = 3$); in principle, they can be calculated ab initio; however, in specific calculations, it is more convenient to consider them parameters; here, it is sufficient to take into account one or two multipoles (20) (see Section III); U(R) in (20) is the classical molecular interaction potential. /15

A highly significant circumstance in the question under consideration, which must be taken into account without fail, is that, *although there is a specific internal connection between* the classical interaction potential U(R), which determines the collision dynamics, and perturbation Δ(R) which determines the shift of the resonance frequencies, these are significantly different functions, which can have noncoinciding analytical approximations. While U(R) takes the effect of molecular interaction on classical variables into account, Δ(R) determines the effect of molecular interactions on the quantum variables.

2.2. Some Consequences of a General Formula /16

Despite the outward complexity of formulas (16) - (24), they permit simple interpretation, and they permit a qualitative explanation of deviations from the dispersion contour and certain other facts which were noted in Section I.

We break down the shifted frequency region into three ranges (see Fig. 3):

I. Region of small disorders of resonance frequencies (central part of line)

$$\Delta\nu \ll \Delta\nu_1. \tag{25}$$

II. Line periphery (region of quasistatistical wings)

$$\Delta\nu_1 \ll \Delta\nu \leqslant \Delta\nu_2. \tag{26}$$

III. Remote wings of line (region of exponential wings)

$$\Delta\nu \gg \Delta\nu_2. \tag{27}$$

The division into these ranges is arbitrary, but it permits features which determine the qualitative form of the frequency distributions of intensity to be distinguished.

The behavior of function $\Phi(R)$ (see (21))is essential to the analysis. The course of this function is given in Fig. 4 (see also Table III), for three sets of parameters ε/kT and σ, when U(R) is modeled by the Lennard-Jones potential (see expression (34)); only this potential is used in this paper). With sufficiently large R, function $\Phi(R)$ approaches one, at smaller distances, $\Phi(R)$ negligibly exceeds this value, and, depending on the parameters, it has a more or less sharply expressed maximum (R corresponds to the attraction branches of classical interaction potential U(R)). With further decrease of (R), a sharp exponential drop is observed (repulsion brancy of U(R)). /17

The region of small disorders of resonance frequencies (1), as follows from expression (22), is connected to the condition

$$C_3^2 \gg 4\Delta\nu^{2\frac{m-3}{m}} C_m^{\frac{6}{m}} (\Delta\nu). \tag{28}$$

An equality in expression (28) gives the frequency shift $\Delta\nu_1$ in relationship (25). According to definition (22), under condition (28), R is sufficiently large, i.e., $\Phi(R) = 1$. With this taken into account, from expressions (22), (20), (19) and (17), we obtain $w(\Delta\nu) = 1$; i.e., the "generalized contour" coincides with the Lorentz contour.

In the regions of the periphery (II) and remote wings (III), we have the inverse inequality of (28) and a result which coincides with that presented in monograph [1].

On the periphery of the line (II), we juxtapose a range of values of $\Phi(R)$, which differ negligibly from 1 (attraction branch and area near the minimum of curve U(R)). For example, we take a value for frequency $\Delta\nu_2$, determined from the relationship

$$R(\Delta\nu_2) = R_0, \tag{29}$$

where R_0 is the solution of the equation

$$\varphi(R_0) = 1. \tag{29a}$$

It follows from expression (22) and Fig. 4 that R_0 depends on the parameters of a specific line of the gaseous mixture. Then, by describing formula (20) in the single multipole approximation (two terms in the denominator), it is easy to determine that, in the region $\Delta\nu_2 \geqslant \Delta\nu \gg \Delta\nu_1$, form factor $f(\nu - \nu_0)$ coincides with the statistical contour ($\Phi(R) \simeq 1$):

$$f(\nu-\nu_0) = \frac{4\pi N_3}{m_3} \frac{C_{m_3}^{3/m_3}}{\Delta\nu^{1+3/m_3}} + \frac{4\pi N_4}{m_4} \frac{C_{m_4}^{3/m_4}}{\Delta\nu^{1+3/m_4}}. \tag{30}$$

/18

On the remote wings of the line (III, $\Delta\nu \geqslant \Delta\nu_2$), the spectral distribution of $f(\nu - \nu_0)$ is determined by the course of functions $\Phi(R)$, i.e., there is an exponential contour.

As is evident from condition (28), the region of mutual transition of the Lorentz contour to the contour according to the theory of the wing developed in [1] depends on line width γ and parameters C_m of the multipoles which modeled the shifts of the resonance frequencies $\Delta(R)$ (see (13)). The boundary of

the transition to a sharply exponential drop $-\Delta\nu_2$ is sensitive to the nature of the multipoles which determine $\Delta(R)$. The inclusion of higher order multipole shifts the boundary of $\Delta\nu_2$ to the region of larger values, which accounts for the multipole interaction spectral dispersion effect. Variations of the parameters of intermolecular potential U(R) can have a severe effect on the boundary of $\Delta\nu_2$, as well as on the steepness of the drop of $f(\nu - \nu_0)$, as is seen from Fig. 4.

The above indicated characteristics of formation of the line contour is brought out easily in numerical calculations.

The results of calculation on the generalized contour in the single multipole approximation, curve C_4 (resonance dipole-quadrupole interaction, $\underline{m} = 4$) and in the double multipole approximation, curve $C_4 + C_5$ (resonance dipole-quadrupole and quadrupole-quadrupole, $\underline{m} = 4$ and $\underline{m} = 5$) and curve $C_5 + C_8$ (resonance quadrupole-quadrupole and nonresonance dipole-quadrupole, $\underline{m} = 5$ and $\underline{m} = 8$), are given by the dashed curve in Fig. 1. The Fig. 1 data are reproduced by Table 1 (similarly for Fig. 2). Since the line has a low resonance frequency of 18.58 cm^{-1}, it is sharply asymmetrical, so that the $\underline{m} = 4$ interaction does not affect the distribution noticeably. The central part of the line (region I of Fig. 3) extends to $\Delta\nu \simeq 5\gamma$, where k_L is 80% of the total value; the "junction" region, from 5γ to 3.82 cm^{-1}, where k_L is little more than 35%; the line periphery (region II) reaches the shifted frequency $\Delta\nu \approx 80$ cm^{-1}, after which region III begins, where the path of the form factor is exponential (cases $\underline{m} = 4$ and 5).

The multipole interaction spectral dispersion effect appears in this figure. Right up to frequency shift 31 cm^{-1},

interaction $\underline{m} = 5$ makes the basic contribution to $f(\nu)$ (at $\Delta\nu = 15.62$ cm^{-1} more than 75% and at $\Delta\nu = 31.42$ cm^{-1}, about 57%); the inclusion of an additional higher order multipole ($\underline{m} = 8$) moves the boundary of the exponential wings more than 200 cm$^{\pm 1}$. At frequency shifts of over 85 cm^{-1}, the contribution of the lower order interaction ($\underline{m} = 4$) can be disregarded. Fig. 1 also illustrates what a substantial discrepency (by an order of magnitude) is observed with expressions (1) - (4) in the line periphery region.

Figure 2 illustrates the regularities brought out in Fig. 1. Since the resonance frequency is more than the preceding by more than a factor of ten, 419.9 cm^{-1}, the asymmetry in the line is highly insignificant. The additional calculations are of interest, curve C_5^* and curve C_8^*, which represent the path of the form factor from the formulas of the remote wing "unjoined" to the Lorentz contour (the actual path of function $\kappa(\nu - \nu_0)$). It is evident that the generalized contour coincides qualitatively with the formulas from the theory of the remote wing of [1]. Attention is attracted to the fact that, in a specific region of shifted frequencies, for example from 6 cm^{-1} to 30 cm^{-1}, the distribution can be approximated by a simple expression, by statistical contour (7), (30), with $\underline{m} = 5$ and error of 17-45% and, /20 in a narrower section with greater accuracy (in this range, curve C_5^* actually is calculated according to contour (7), since $\Phi(R) \approx 1$ for these frequency shifts).

Thus, a situation can occur in molecular spectra, when the general distribution relative to the complex functional form appears at some frequencies, in the form of a simple analytical approximation of the type of (8) or (9) (see also Figs. 7, 9, Section 3).

A comparison of Fig. 1 and Fig. 2 also shows the effect of change in line parameter γ on the position of the "junction" region shown in Fig. 3. With change in line half width from 0.111 cm^{-1} to 0.06 cm^{-1}, i.e., with almost a two-fold decrease in γ, the "junction" region is shifted very substantially, from $3.82\ cm^{-1} > \Delta\nu_1 > 5\gamma$ to $5\gamma > \Delta\nu_1 > 2\gamma$. Frequency shift $\Delta\nu_2$, which arbitrarily divides the region of quasistatistical and exponential distributions, is practically unchanged, and it lies in the 180 cm^{-1} - 315 cm^{-1} range.

We single the most important consequences.

1. Type (8), (9), (10) approximations found in the experiments of various authors are partial cases of a more general distribution in specific frequency shift ranges, and they depend on the type of absorbing component and gaseous mixture.

2. At sufficiently great distances from the line or band center, an exponential drop of intensity should be observed, regardless of the spectral range of the line or band, from the specific absorbing and buffer gas.

3. It follows from indirect calculations (see Fig. 1, 2 and Tables 1, 2) that, at small and intermediate frequency shifts, the generalized contour results in higher values of the form factor of the line than the Lorentz contour and, only in proportion to the shift to the remote wing does $f(\nu - \nu_0)$, in accordance with (16), lie significantly lower; in this case, the values from the two contours differ by a factor of ten. /21

4. A highly interesting consequence of expressions (16) - (24) is the dependence of the self-broadening effect on the

frequency shift region under consideration.

As is known, for Lorentz line contour (1), the self-broadening coefficient is determined by the relationship

$$\sigma_{sf} = \gamma_s / \gamma_f \tag{31}$$

and, by definition, it does not depend on the frequency shift. With $\Delta\nu > \gamma_s = \gamma + \gamma_f$, relationship (31) can be rewritten in the form

$$\sigma_{sf} = \frac{k_s^{(L)}(\Delta\nu)}{k_f^{(L)}(\Delta\nu)} \equiv \frac{\gamma_s}{\gamma_f}. \tag{32}$$

By analogy with (32), we introduce the self-broadening coefficient for contour (16)

$$\sigma_{sf}(\Delta\nu) = \frac{k_s(\Delta\nu)}{k_f(\Delta\nu)} \equiv \frac{\varkappa_s(\Delta\nu)}{\varkappa_f(\Delta\nu)}. \tag{33}$$

Since, for the cases of self-broadening and broadening by an extraneous gas, the types of multipoles utilized change and, moreover, they develop irregularly with change in frequency shift (the multipole interaction spectral dispersion effect), self-broadening coefficient (33) is a function of frequency.

As was shown in [1], for a H_2O - N_2 mixture, self-broadening

coefficient $\sigma_{sf}(\Delta\nu)$ can change by an order of magnitude, with removal to the wing of the line. Fig. 5 and Table 4 reflect the nature of the self-broadening coefficient vs. $\Delta\nu$ for a $CO_2 - N_2$ mixture, in a case of a line with parameters characteristic of the "strong line approximation") in the 4.3 μm band (see Section 3). According to formula (31), $\sigma_{sf} = 1.06$. With increase in disorder of the resonance frequency, in accordance with definition (33), $\sigma_{sf}(\Delta\nu)$ increases to 3.51, i.e., by 3.3 times, at $\Delta\nu = 50.7\ cm^{-1}$, and it then decreases to 0.89, at $\Delta\nu = 200.7\ cm^{-1}$. /22

In summarizing what has been presented in this section, it can be concluded that the generalized line contour represents the basic physical regularities which result in its broadening and, on the qualitative level, it permits a relatively simple interpretation of the complicated and, at first glance, contradictory picture of the frequency distributions of intensity on a line and band periphery. This permits the hope for high efficiency of the approximate formulas with a small number of parameters based on it, for quantitative calculations.

3. Quantitative Interpretation of Radiation Absorption in the 4.3 μm, 2.7 μm, and 1.4 μm Carbon Dioxide Bands

3.1. Calculation Procedure and Initial Information /23

Any quantitative calculations for analysis of vibration-rotation spectra are extremely laborious work. Therefore, the problem of their optimization becomes of paramount importance, and it should be solved from the viewpoint of their goals. The purpose of our work was to verify the efficiency of the theory from the point of view of quantitative interpretation of anomalies of the absorption coefficient in the wings of the vibration-rotation bands of carbon dioxide and to determine the

possibilities of introduction of the enitire set of empirical data of simple formulas with a small number of parameters for quantitative interpretation, i.e., the problem of complete quantitative reproduction of each specific example was not undertaken, although this possibly should be the next stage of the work (see Section 4).

The initial information required for the use of formulas (16) - (24) includes the line parameters (ν_0, S and γ), the form of the classical molecular interaction potential and the parameters which characterize it, and the set of constants C_m, which define the shift of the resonance frequencies.

The location of the line center (ν_0), and its integral intensity (S) and half width (γ) are the traditional objects of spectroscopic studies and, accordingly, there is a very extensive literature. Systematization of the data presented in [34] is the most complete. This was the basis for its use in the calculations carried out below.

Information on intermolecular potentials is highly contradictory. The widespread method of analysis assumes a priori assignment of the analytical form of the potential, /24 and the problem usually is reduced to finding their parameters [35,36]. It is significant that the selection of models in this case, as a rule, is dictated by the convenience of mathematical description. Available information does not permit an unambiguous choice to be made [35, 36]. Thus, it is highly reasonable to use the simplest potential with a minimum of parameters as the first step. The Lennard-Jones potential was used in our calculations:

$$U(R)=4\varepsilon\left[\left(\frac{\sigma}{R}\right)^{12}-\left(\frac{\sigma}{R}\right)^{6}\right]. \qquad (34)$$

The specific nature of functions U(R) and Δ(R) has been noted (see p. 16). We add that, in contrast to U(R), modeling of the type of Δ (R) is necessary in setting up the problem of calculation of the spectra of the correlation functions. As was shown in [1], representation of Δ(R) in the form of a multipole series is valid for $R > R_0$, where R_0 is on the order of molecular dimensions. Moreover, representation (13) permits a solution to be obtained in sufficiently general form. Of course, the change to specific calculations assumes a limitation on the summing in expressions (20). It is known that, in calculation of γ [7, 37], the use of the first, more rarely the first two terms in the multipole expansion usually is sufficient. This can be explained, since the intermolecular distances at which broadening occurs are much greater than R_0. In shaping the contour of larger frequency shifts, the utilization of the distances characteristic of the repulsion branch is possible, i.e., approximation Δ(R) includes practically the same range of R as U(R). The difficulty which arises here is completely like the difficulties of analytical representation of U(R). While there is approval of the form of U(R) in different problems, although it is quite controversial, information on Δ(R) is completely lacking today. The use of /25 the mathematically simplest alternate version

$$\Delta(R) = \frac{C_m}{R^m} + \frac{C_k}{R^k}; \quad (m < k); \tag{35}$$

where m, k and C_m, C_k are certain unknown parameters (according to the remark on page 16, they do not have to coincide with the parameters of the Lennard-Jones potential without fail), seems logically justified. As the calculations show, the use of the first term in (35) may prove to be

completely sufficient. It should be noted that the joining procedure used in Section 2, which is reflected in the form of expressions (20) and (22), actually means the use of approximation $\Delta(R)$ in the form

$$\Delta(R)=\frac{C_3}{R^3}+\frac{C_m}{R^m};\quad (m>3), \tag{36}$$

The first stage of the calculations included the use of the "strong line approximation," in finding the most probable ranges of values of $\underline{m}$ and C_m. Line-by-line calculation was then carried out, with account taken of the structure of the specific vibration-rotation band, but assuming the values of γ, $\underline{m}$ and C_m to be independent from line to line.

We dwell on the procedure of calculations in the "strong line approximation." The absorption coefficient at frequency ν is determined by the relationship

$$k(\nu)=\sum_i k_i(\nu)=\sum_i S_i f_i(\nu-\nu_i), \tag{37}$$

where $k_i(\nu)$ is the absorption coefficient at frequency ν due to the i-th line in the band and the summation is carried out over all lines. We assume the presence of a rather large number of lines, in which their distribution is such that, from summing (37), we can proceed to integration. Then, with the /26

use of the theorem of the mean, there can be rewritten

$$k(\nu) = k_{i*}(\nu) = S_{i*} n \varphi_{i*}(\nu - \nu_{0i*}). \tag{38}$$

That is to say, the absorption coefficient at frequency ν is determined by the absorption coefficient of some effective line in the band with center ν_{0i*}, with integral intensity $S_{i*}n$ (n is the number of lines of the band which contribute to $k(\nu)$), half width γ_{0i*} and multipole constants m_{i*} and $C_m^{(i*)}$.

As an example, we present the formula used in [1, 38], for interpretation of the experimental results. We make use of the fact that we are interested in quite large frequency shifts, i.e., inverse condition (28) is valid. Then, in the single multipole approximation, the following can be written

$$k(\nu) = S \frac{\beta \varphi(R)}{|\nu - \nu_0|^{1+3/m}}. \tag{39}$$

Expression (39) is consistent with formula (21) in [38](see also [1]). In (39),

$$R = \left(\frac{C_m}{|\nu - \nu_0|}\right)^{1/m} \quad (A); \qquad \beta = \frac{4\pi N}{m} (\tilde{C}_m)^{3/m}, \quad (B).$$

Constants C_m and $\tilde{C}_m$ are different in (A) and (B), by virtue of the intermediate transformations

$$S_{i*} n \frac{4\pi N}{m} C_m^{3/m} \equiv S\beta \equiv S \frac{4\pi N}{m} (\tilde{C}_m)^{3/m}; \tag{40}$$

according to (40)

$$\tilde{C}_m = C_m \left(\frac{n S_{i*}}{S} \right)^{m/3} \qquad (41)$$

It was assumed in (40) that $C_m^{(i*)}$ identically $\underline{m}$, $\nu_{0i*} \equiv \nu_0$. /27
Expression (39) has four parameters (ν_0, $\underline{m}$, β, C_m). The number of parameters in [1, 38] was decreased, because it was assumed that ν_0 was the center of the band and that the quadrupole-quadrupole resonance ($\underline{m}$ = 10) is the decisive multipole. The results of calculation by formula (31), with constants taken from [38], are presented in Fig. 8a and Table 8.

The use of expressions similar to (39) in this paper seemed inadvisable for two reasons. First, inverse condition (28) is not satisfied for the high frequency wing of the 1.4 μm band, while the procedure has to be the same for all bands. Second formula (39) proves to be of little use in changing to line-by-line calculations, since ambiguity develops in the selection of approximate values of parameter C_m (the values of C_m, recovered from β and R, prove to be very different).

The formula for the "strong line approximation," by which the calculations were carried out, had the form

$$k(\nu) = S\varphi(\nu - \nu_0) = \frac{S}{\pi} \frac{\gamma \varphi(R)}{(\nu-\nu_0)^2+\gamma^2} \frac{\left(1+\sqrt{1+4\Delta\nu^2 \frac{m-3}{m} C_m^{\frac{6}{m}}/C_3^2}\right)^2}{1+\frac{m}{3}\frac{C_m}{C_3}R^{3-m}}, \qquad (42)$$

where

$$R = \left\{ \left(C_3 + \sqrt{C_3^2 + 4\Delta\nu^2 \frac{m-3}{m} C_m^{\frac{6}{m}}} \right) / 2\Delta\nu \right\}^{1/3}; \quad C_3 = \frac{3\gamma}{4\pi^2 N_L}. \qquad (43)$$

Expression (42) follows from (16) - (24), for the case of a

single component mixture or for the case $N_s << N_f$. The factors in expression (17) differ extremely little from 1 in the region under consideration.

The following were used in the calculations: ν_0, the position of the vibrational transition frequency for a given band; S, its integral intensity; γ was assumed to be 0.07 cm^{-1}, in the case of CO_2 - CO_2, and 0.066 cm^{-1} for the CO_2 - N_2 mixture. Constants $\underline{m}$ and C_m were variable parameters. /28

To find $\underline{m}$ and C_m, a scheme based on the tendency displayed in the multipole interaction spectral dispersion effect was used. The inclusion of higher order multipoles at large frequency shifts increased the absorption coefficient considerably more sharply. A graph of the absortion coefficient vs. frequency shift was plotted. Two points were plotted on the graph, which correspond to $k(\nu)$ at the minimum and maximum frequencies recorded in the experiment for a given vibration-rotation band. Then, $\underline{m}$ was recorded and $C_m^{(max)}$ was determined for it, based on the fact that, at $\Delta\nu = \gamma$, the absorption coefficient did not go beyond 10% of the value calculated on the Lorentz contour. Subsequent calculations were carried out for the two frequencies indicated above. If the calculated absorption coeffients exceeded the experimental at the two frequencies, the calculation was repeated with reduced C_m, until the following situation was reached: $k(\nu_{min}) > k_{exp}$ and $k(\nu_{max}) > k_{exp}$ or $k(\nu_{min}) \lesseqgtr k_{exp}$ and $k(\nu_{max}) < k_{exp}$. Further calculations were carried out for larger $\underline{m}$, and which $\underline{m}$ gives the best approximation to the experiment was checked. If it turned out that the increased $\underline{m}$ was preferable, calculation was repeated with still larger $\underline{m}$.

As has been pointed out, after finding $\underline{m}$ and C_m, a line by line calculation of the absorption coefficient was carried out according to expression (37), based on formula (42), for which ν_{oi} and S_i were taken from the atlas of [34], line half width /29

γ and constants $\underline{m}$ and C_m were considered to be the same for all lines in the band.

3.2 Calculated Results

Figure 6 (see Table 5) illustrates the method of finding parameters $\underline{m}$ and C_m for the 4.3 μm band in the self-broadening case. In the part of the figure which corresponds to larger frequency shifts, the coefficient of absorption, found in [3] for frequencies 2400 cm^{-1} and 2550 cm^{-1}, are noted by the symbol $\underline{x}$. The three curves correspond to three multipole approximations. It is evident that it is impossible to interpret the experiment by variations of C_5. The use of multipole $\underline{m}$ = 10 improves the situation, permitting an approach to experiment at a frequency of 2400 cm^{-1}, but the discrepency at 2550 cm^{-1} remains very significant. Multipole $\underline{m}$ = 20 proves to be extremely fortunate, but further increase does not improve the result.

Figure 7 (see Table 6) is indicative. Results are given in it, of the calculation in the "strong line approximation" for the Lorentz contour, the modified Lorentz contour (9) proposed in [2] (its parameters for the 4.3 μm band were calculated in [2] in the "strong line approximation") and generalized line contour (42). The very much better agreement of contours (9) and (42) in the measurement region is evident. We note that empirical approximation (9) has three parameters, while (42) has two parameters.

Figure 8 (see Table 7) gives the results of calculations of the high frequency wings of the 4.3 μm, 2.7 μm and 1.4 μm bands for the self-broadening case, in the "strong line approximation" and with line-by-line calculation, and curves also are plotted on the graphs which approximate experiment from the data of [3].

As should be expected, the change to the line-by-line calculation scarcely shows up at high frequencies, and the band structure clearly has to be taken into account at small ν (an increase in /30 values of $k(\nu)$, of more than two times for the 4.3 μm and 1.4 μm bands and nearly 1.5 times for the 2.7 μm band). On the whole, quite good agreement with experiment should be noted; however, the generalized contour in the 1.4 μm band gives a sharper drop of the absorption coefficient.

Figure 9 (Table 8) gives the results of calculations in the "strong line approximation" for the 4.3 μm band, in the case of broadening by molecular nitrogen, on three contours: Lorentz, empirical (9) and generalized. As in the self-broadening case, the agreement of distribution (9) and the generalized contour in the measurement region is quite good.

Figure 10 (Table 9) presents data on the three 4.3 μm, 2.7 μm and 1.4 μm bands for a CO_2 - N_2 mixture. As for self-broadening, the change to line by line calculation shows up significantly, only at lower frequencies for the first two bands.

The curve of the results in the "strong line approximation" for the 1.4 μm band is absent in Fig. 8c. Since the spectral measurement range is quite narrow, 20 cm^{-1} (for CO_2 - CO_2, 100 cm^{-1}) and still closer to the edge of the band than in the case of CO_2 - CO_2, by 10 cm^{-1}, the change to line by line calculation extremely strongly changed the results of calculation in the "strong line approximation" (by a factor of ten at the next frequency). For this reason, parameter m was not found specially for the 1.4 μm band, but it was assumed to be 30. Agreement with test data is extremely satisfactory in the 4.3 μm and 2.7 μm bands. However, in the 6990-7000 cm^{-1} frequency region, the discrepency is extremely significant (almost fourfold at 6990 cm^{-1}).

We discuss some consequences of the calculations.

The fact that the periphery and remote wings are significantly different in the self-broadening cases and with broadening by an extraneous gas, especially compared with the central part of the line, attracts attention. Fig. 5 (Table 4) is significant in this respect. It presents absorption coefficient calculation data for the line with parameters taken from the "strong line approximation" in the 4.3 μm band, for CO_2 - CO_2 and CO_2 - N_2 mixtures (actually, the behavior of the form factors of the lines for the two mixtures, at identical concentrations of the broadening gas, is represented in the graph, since the same integral intensity was used in both calculations; for complete coincidence of Fig. 5 with the form factor graph, it is sufficient to change only the values of the record points, while preserving the ordinate scale). Up to frequency shifts on the order of a few cm^{-1}, they differ extremely insignificantly; however, at larger $\Delta\nu$, the discrepancy becomes highly noticeable. /31

The regularities noted can be given the following interpretation. According to the data of [3], self-broadening coefficient $\sigma = \gamma_s/\gamma_f$ differs extremely negligibly from one (1.22). This is because the same multipole interactions, resonance quadrupole-quadrupole, $\underline{m} = 5$ [39] contribute to broadening of the central part of the line, in both the CO_2 - CO_2 and CO_2 - N_2 cases, and they show up only in the parameter of the contour, and not in the frequency distribution itself. The situation changes on the periphery. The behavior of function $\Phi(R)$, which depends on the intermolecular potential, has an appreciable effect on the frequency form factor. The parameters of potential (34) are different for these two cases:

$\varepsilon/k = 190°K$, $\sigma = 4$ Å (CO_2 - CO_2), $\varepsilon/k = 132°K$; $\sigma = 3.8$ Å (CO_2 - N_2).

Besides, as is shown by the results of regeneration of data of $\underline{m}$, the resonance frequency shift in the area of the line periphery is described by different functions ($\underline{m}$ = 20 (CO_2 - CO_2) and $\underline{m}$ = 30 (CO_2 - N_2)), which indirectly affects the frequency.

We comment on the data obtained on parameter $\underline{m}$. Different values of $\underline{m}$ for different types of broadening gases are not unexpected, since this is based on causes which are similar to those, which result in different values of the parameters of the classical interaction potential. The quite high values of $\underline{m}$ attract attention. Without yielding to a detailed discussion of this question, we make several remarks. During the calculations, it was easy to determine that the numerical values of the absorption coefficient on the periphery of a band are sensitive to the numerical values of the potential parameters (see comparison of the self-broadening and extraneous gas broadening cases), and they respond to a still greater extent to change in its analytical form. This is particularly noticeable, when molecular interactions appear in the broadening, at the distances characteristic of the repulsion branches of potential U(R). It is easy to change the form of potential U(R) (especially with the ambiguity of available information taken into account), so that parameter $\underline{m}$ has lower values, with practically the same accuracy of description of the test data as a whole. However, this hardly makes sense, for two reasons: first, we have the goal of obtaining approximation of the contour, assuming the mathematically simplest alternate version with a minimum of parameters and that the data used completely satisfies this requirement; second, there is no basis for considering that the steep slope of the function which describes the resonance frequency shift has to be close to the Lennard-Jones potential; moreover, there are indications that, in the case of the gases under consideration, the use of a different model for U(R), which has a larger derivative in the repulsion branch region, for example, the Bukengem potential or the Kikhar potential [35, 36], may prove to be preferable for

/32

specific problems.

It is particularly necessary to single out disagreements between the empirical data and the data of the calculation presented for the region near the edge of the 1.4 μm band. /33 A distinguishing feature of this region is that the measurements were carried out near a group of strong lines. The distance from the edge of this band, where the line intensity in total differs from the maximum by a factor of ten, to frequency 6990 cm^{-1} is 1.61 cm^{-1}, and distance to the most intense line in R branch is 7.93 cm^{-1}. (For comparison, in the wing of the 4.3 μm band, the distance from the minimum frequency 2400 cm^{-1}, at which measurements were carried out, to the most intense line in the R branch is over 30 cm^{-1}.) That is, the accuracy of assignment of the line form in small disorders of the resonance frequency can have an appreciable effect on the value of the absorption coefficient. In this papar, decreases below the Lorentz contour become noticeable, as follows from Figs. 7 and 9 and Tables 6 and 8, at frequency shifts of 6-15 cm^{-1}. On the other hand, the authors of [3] point out deviations of the contour in molecular nitrogen broadening from the self-broadening contour, which they noted, toward lower values, in the first case, at distances of 0.5 cm^{-1} from the center of the line, i.e., in the region of the central part of the line, according to the classification used in Section 2. The validity of the Lorentz contour was not subject to doubt in the results presented.

The basis conclusion from the series of calculations is reduced to a quite high effeciency of the theory developed in [1, 33, 38] and of the generalized contour based on it.

The theory permits an understanding of the physical mechanisms which control the shaping of the line contour. The

line contour permits calculation to be carried out in random disorders of the resonance frequencies, and, by means of simple formulas with few parameters overall, a satisfactory description of present experimental material, and removal of the disagreements between theory and experiment which have existed so far, and which have become on the order of the measured values of the absorption /34
coefficients.

In concluding this section, we note again that the contours proposed in experimental works [3, 29] and which have become widespread in actual calculations have three and four parameters, respectively, in which all the parameters change in changing from band to band. At the same time, the generalized line contour has two parameters. In this case, the position of the band in the spectrum shows up, only in changes of one parameter.

4. Further Research

Progress in understanding the regularities which determine /35
line form in random disorders of resonance frequencies and the possibility of the elimination of serious disagreements between theory and experiment on the frequency variation of the absorption coefficient, based on relatively simple formulas with few parameters, permits the raising of the question of investigation of finer effects, which are extremely important from the point of view of satellite sounding, and the problem of further increase in accuracy of analytical approximations. Questions are formulated below, which, in our opinion, require serious theoretical and experimental work. They are grouped around three areas:

1. Study of the temperature dependence of the absorption coefficient on the periphery of spectral lines;

2. Working out of formulas which permit calculation of the line form factor in random disorders of the

resonance frequencies, with no less accuracy than the accuracy of experimental measurements;

3. Further testing of the efficiency of the approach developed, from the point of view of determination of possibilities of prediction of molecular absorption in other spectral ranges and vibration-rotation bands.

4.1. Temperature Dependence

According to (19), (21) and (42), with a constant concentration of the broadening molecules, the temperature dependence is determined by function $\Phi(R)$. At intermolecular distances $R > \sigma$, the exponent of subintegral expression (21) is $\underline{u}(R)/kT$. Correspondingly, at shifted frequencies connected with these R (see relationships (22), (43)) with increase in temperature functions $\Phi(R)$ and consequently the line form factor decrease. With large $\Delta\nu$, a situation occurs, when $R < \sigma$. In this region of $\Delta\nu$, the pattern of the temperature dependence changes to the reverse. With increase of T, the form factor should increase, since $U(R) > 0$. Fig. 4, on which curves are presented for two temperatures, confirms what has been stated. /36

In Fig. 11 (Table 10), the results of calculation of the absorption coefficient beyond the edge of the high frequency wing of the 4.3 μm carbon dioxide band, with self-broadening at two temperatures, 300° K and 213° K (curves 1, 2), are presented. It is evident that, with decrease in temperature, the absorption coefficient drops quite sharply. Data of experimental studies in the 2400 cm^{-1} - 2460 cm^{-1} spectral range are presented in this figure (curves II and III). They give the opposite relationship. There also are indications of a similar variation in the temperature dependence in [3].

It is not possible to give a strict interpretation of this contradiction. We express one possible hypothesis. In Fig. 11, curves 3,4 and 5 present the results of calculations at T = 213° K, but with a change in value of the parameters of the potential, ε and σ. Small reductions of them have a drastic effect on the behavior of the absorption coefficient. Curve 4 is particularly significant in this respect. A change of σ from 4 A to 3.95 A, i.e. by 0.05 A, produces the required variation in the temperature dependence. On consideration that the calculations in Fig. 11 were in the " strong line approximation," and the fact that the change to line by line calculation increases the value of $k(\nu)$ from one and a half to two times, it can be considered that such small changes in the parameters of the potential, ε and σ (curve 5), give, besides a qualitative, a good quantitative agreement.

We do not know of any experimental recordings of the parameters of the intermolecular potential vs. temperature, although current ideas of the origin of the forces of molecular interactions, in principle, permit such a connection to be hoped for [35, 36]. It also is noteworthy that, for a quantitative interpretation of /37 an experiment, small variations of σ and ε are necessary, which are considerably smaller than the scatter of these parameters regenerated by various procedures [35].

It appears necessary to conduct additional experiments, in order to confirm the results of [4], as well as to expand the region of frequency shifts under study. It is easy to see from Fig. 11 that approximation of the absorption coefficient by the empirical formula of [4] in the region of large frequency shifts (the region beyond the vertical dashed line) contradicts the data of other authors. It also is desirable to determine the temperature dependence experimentally, at intermediate small frequency shifts. Experiments in different bands are necessary, to answer the question as to the source of the temperature anomalies.

Are they of the nature of inaccuracies in the initial information, or do they result from imperfections of the mathematical model of the contour.

This question is all the more important, as to the characteristics which are the object of sounding.

4.2. Problems of Increasing Approximation Accuracy

Ways of increasing the accuracy of approximations within the methodology developed involves correction of approximation [36] for $\Delta(R)$, as well as testing the validity of the Lorentz contour in the regions of small $\Delta\nu$. As follows from Tables 7 and 9, where data on all bands are presented, and from the results of the discussions of Sections 2 and 3, this should show up primarily in the intermediate 1 - 20 cm^{-1} frequency shifts. Progress is delayed here by the lack of reliable data which could be a control for the theoretical constructions. In this part of the investigation, the main support must be the conduct of carefully thought out experiments. Evidently significant progress could be made here by /38 direct, high resolution measurements (no more than fractions of the line width) of the contour of the spectrum, even if in a single limited spectral range, which includes only two lines at a distance of at least a few of their widths from each other (distances up to 1 - 2 cm^{-1} are desirable), in one of the bands under consideration. In connection with this, in all likelihood, it is necessary in the theoretical studies to formulate the problem of selective absorption by lines, against a background of strong absorption, and of extraction of the corresponding background.

Of course, questions of increasing the accuracy of approximations should include questions of the accuracy of the a priori information.

It is not excluded that the appearance of additional empirical data would require refinement of the mathematical model of the wing. By virtue of the considerable success in interpretation of the frequency distributions which were discussed in this paper, it is to be hoped that it will be just refinements, and not fundamental changes in the approach developed.

4.3. Further Verification of Efficiency of Approximations Suggested

The practical efficiency of a given analytical approximation, in the final analysis, is determined by achievement of the finite goal which had to be established in this paper, namely, achievement of the accuracy of calculation of the weighting functions, which is required in satellite temperature sounding. There are no such estimates for the proposed expressions. It seems advisable, at this stage of analytical approximations, to include them in calculation of the absorption functions and weighting functions for two bands: 4.3 μm and 15 μm. Based on data for the 4.3 μm band, correlative connections could be established between the error of approximation of the absorption coefficient and the accuracy of calculation of, for example, the weighting functions. Calculations in the 15 μm band, according to various contour forms, /39 and comparison with empirical spectra would be an estimate of the predictive power of the theory, when data on the band under study are not used in finding the parameters of the contour. Such calculations would be extremely informative, if they are carried out under measurement conditions completely coincident with the thermodynamic conditions (without intermediate recalculation) and with the parameters of the spectroscopic equipment.

In conclusion, the most important conclusion should be recorded: the fruitfulness of further developments connected with increasing reliability of information on line form is

practically completely dependent on the coordination of the experimental and theoretical study programs conducted and of their mutual tie in.

REFERENCES

1. Nesmelova, L.I., S.D. Tvorogov and V.V. Fomin, Spektroskopiya kryl'yev liniy [Line Wing Spectroscopy], Siberian Section, Nauka Press, Novosibirsk, 1977.

2. Winter, B.N., S.S. Silverman and W.S. Benedict, "Line shape in the wing beyond the band head of the 4.3 μm band of CO_2," J. Quant. Spectrosc. and Radiat. Transfer 4/4, 527-538 (1964).

3. Burch, D.E., D.A. Gryvnak, R.R. Patty and C.E. Bartky, "Absorption of infrared radiant energy by CO_2 and H_2O. IV. Shapes of collision-broadened CO_2 lines," J. Opt. Soc. Am. 59/3, 267-280 (1969).

4. Bulanin, M.O., V.P. Bulychev, P.V. Granskiy, A.P. Kouzov and M.V. Tonkov, "CO_2 transmission function in the 4.3 and 15 micron regions," in the collection Problemy fiziki atmosfery [Problems of the Physics of the Atmosphere], No. 13, 1976, pp. 14-24.

5. Zuyev, V.Ye., Rasprostraneniye vidimykh i infrakrasnykh voln v atmosfere [Propagation of Visible and Infrared Waves in the Atmosphere], Sov. radio Press, Moscow, 1970.

6. Goody, R.M., Atmosfernaya radiatsiya, ch. I. Osnovy teorii [Atmsopheric Radiation, Part I. Theoretical Foundations], Mir Press, Moscow, 1966.

7. Tsao, C.J. and B. Curnutte, "Line-widths of pressure-broadened spectral lines," J. Quant. Spectrosc. and Radiat. Transfer 2/1, 41-91 (1962).

8. Lorentz, H., Proc. Amsterd. Acad. Sci. 8, 591 (1906).

9. Van Vleck, J.H., "The absorption of microwaves by uncondensed water vapour," Phys. Rev. 71/7, 425 (1947).

9x. Van Vleck, J.H. and H. Margenau, "Collision theories of pressure broadening of spectral lines," Phys. Rev. 76/8, 1211-1214 (1949).

10. Zhevakin, S.A. and A.P. Naumov, "Coefficient of absorption of electromagnetic waves by water vapor in the 10 μm-2 cm range," Izv. vuzov. Radiofizika 10/9-10, 1213-1243 (1967).

11. Zuyev, V.Ye., S.D. Tvorogov and V.V. Fomin, "Theory of spectral line broadening and absorption band countour formation," collection Prikladnaya spektroskopiya [Applied Apectroscopy], Institute of Physics, Academy of Sciences Belorussian SSR, Minsk, 1974, pp. 41-65.

12. Alekseyev, V.A. and I.I. Sobel'man, "Some specific features of the broadening of overlapping spectral lines," Preprint No. 58, Physics Institute USSR Academy of Sciences, Moscow, 1968.

13. Burshteyn, A.I., M.L. Strekalov and S.I. Temkin, "Spectral exchange in rotational structure collision broadening," ZhETF 66/3, 894-906 (1974).

14. Alekseyev, V.A., T.L. Andreyeva and I.I. Sobel'man, "The quantum kinetic equation method for atoms and molecules and its application to calculation of the optical characteristics of gases," Preprint No. 124, Physics Institute USSR Academy of Sciences, 1971.

15. Zuyev, V.Ye. and M.V. Kabanov, Perenos opticheskikh signalov v zemnoy atmosfere (v usloviyakh pomekh) [The Transfer of Optical Signals in the Earth's Atmosphere (Under Noise Conditions)], Sov. radio Press, Moscow, 1977.

16. Bignell, K.J., "On the water vapour infrared continuum," J. Roy. Met. Soc. 96/409, 390-403 (1970).

17. Ryadov, V.Ya. and N.I. Furashov, "Spectrum of radio wave absorption by atmospheric water vapor in the 1.15-1.5 mm range," Izv. vuzov. Radiofizika 15/10, 1469-1474 (1972).

18. Sobel'man, I.I., Vvedeniye v teoriyu atomnykh spektrov [Introduction to the Theory of Atomic Spectra], Fizmatgiz Press, Moscow, 1963.

19. Chen. Sh. and M. Takeo, "Spectral line broadening and shift produced by extraneous gases," UFN 66/3, 391-474 (1958).

20. Abels, L.L. and L.M. De Ball, "Deviation from Lorentzian shape in the wings of collision-broadened infrared absorption line of NO," J. Quant. Spectrosc. and Radiat. Transfer 13/7, 663-667 (1973).

21. Traffton, L., "Ammonia line profiles: on deviations from the Lorentz shape," J. Quant. Spectrosc. and Radiat. Transfer 13/7, 821-822 (1973).

22. Traffton, L., "A semiempirical model for the mean transmissions of a molecular band and application to the 10 μ and 16 μ bands of NH_3," Icarus 15/1, 27-38 (1971).

23. France, W.L. and D. Williams, "Total absorption of ammonia in the infrared," J.Opt. Soc. Amer. 56/1, 70-74 (1966).

24. Walsh, T.E., "Infrared absorption of ammonia 20-35 microns," J. Opt. Soc. Amer. 59/3, 261-266 (1969).

25. Varanasi, P. and L.A. Pugh, "Laboratory measurements of absorption by ammonia around 5 microns," J. Quant. Spectrosc. and Radiat. Transfer 13/11, 1225-1228 (1973).

26. Benedict, W.S., R. Herman, G.E. Moore and S. Silverman, "The strength, widths and shapes of lines in vibration-rotation bands of CO," Astrophys. J. 135/1, 277-297 (1962).

27. Varanasi, P., S.K. Sarangi and G.D. Tejwani, "Line shape parameters for HCl and HF in a CO_2 atmosphere," J. Quant. Spectrosc. and Radiat. Transfer 12/5, 857-872 (1972).

28. Varanasi, P., "Shapes and widths of ammonia collision broadened by hydrogen," J. Quant. Spectrosc. and Radiat. Transfer 12/9, 1283-1291 (1972).

29. Moskalenko, N.I., O.V. Zotov and S.O. Mirumyants, "Parameters of spectral lines in the CO_2 absorption bands," collection Tezisov dokladov "II-oy Vsesoyuznyy simpozium po molekulyarnoy spektroskopii vysokogo i sverkhvysokogo razresheniya" [Summaries of Reports, II All-Union Symposium on High and Ultrahigh Resolution Molecular Spectroscopy], Novosibirsk, 1974, pp. 56-58.

30. Schulze, A.E. and C.W. Tolbert, Nature 200/4908, 747-750 (1963).

31. Hill, I.R. and D. Steele, "Vibration band contours. The wings of vibrational absorption bands," Chem. Physics Letters 41/1, 49-51 (1976).

32. Strelkov, G.M., "Changes of line form of linear harmonic oscillator in the kinetic equation method," paper to XII All-Union Conference on Radiowave Propagation, Tomsk, 1978.

33. Fomin, V.V., "Effect of spectral dispersion of multipole interactions on the periphery of spectral lines," Optika i spektroskopiya (in press).

34. McClatchey et al, "Atmospheric absorption line parameters compilation," AFCRL-TR-73-0096, Environment research papers No. 434.

35. Hirschfeld, J., C. Curtis and R. Byrd, Molekulyarnaya teoriya gazov i zhidkostey [Molecular Theory of Gases and Liquids], Foreign Literature Publishing House, Moscow, 1961.

36. Fertsiger, J. and G. Kaper, Matematicheskaya teoriya protsessov perenosa v gazakh [Mathematical Theory of Transport Processes in Gases], Mir Press, Moscow, 1976.

37. Birnbaum, G., "Microwave pressure broadening and its application to intermolecular forces," Advanc. Chem. Phys. 12, 487-548 (1967).

38. Zuyev, V.Ye., L.I. Nesmelova, S.D. Tvorogov and V.V. Fomin, "Theory of spectral line wings and its connection with the problem of the absorption and emission of light by atmospheric gases," Preprint No. 18, Institute of the Optics of the Atmsophere, Siberian Section, USSR Academy of Sciences, Tomsk, 1976.

39. Yamamoto, C., M. Tanaka and T. Aoki, J. Quant. Spectrosc. and Radiat. Transfer 9, 371 (1969).

Appendix 1. Figures

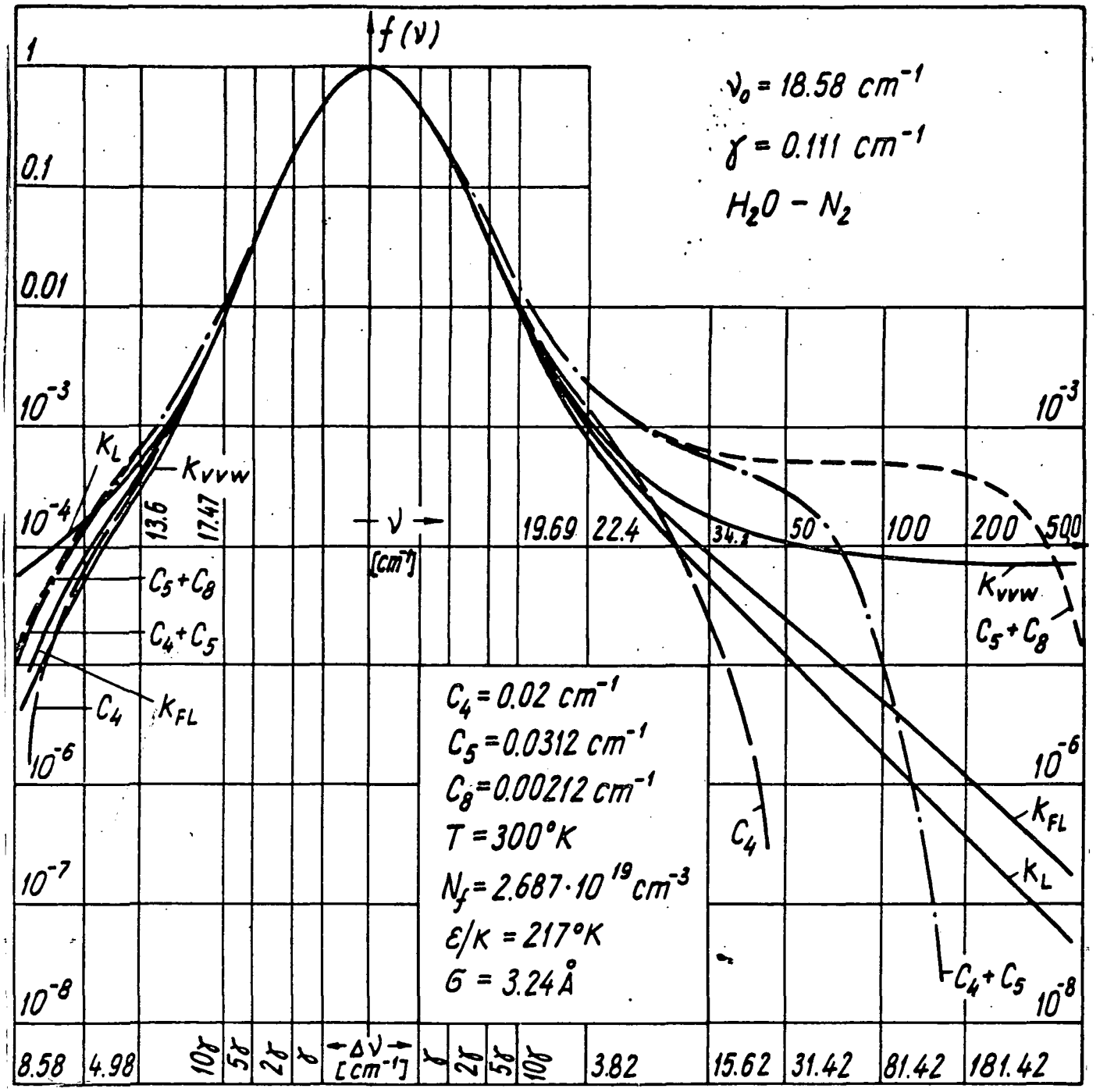

Figure 1. Line form factor f(ν) vs. frequency ν and frequency shift Δν for various contours: solid curves, form factor according to Lorentz contour (k_L), "complete" Lorentz contour and contour according to kinetic equation (k_{FL}), "Van Vleck-Wiesskopf" contour" (k_{VVW}); dashed curves, form factor according to "generalized line contour" with varied modeling of resonance frequency shift; resonance dipole-quadrupole (C_4), resonance dipole-quadrupole and quadrupole-quadrupole ($C_4 + C_5$), resonance quadrupole-quadrupole and nonresonance dipole-quadrupole ($C_5 + C_8$).

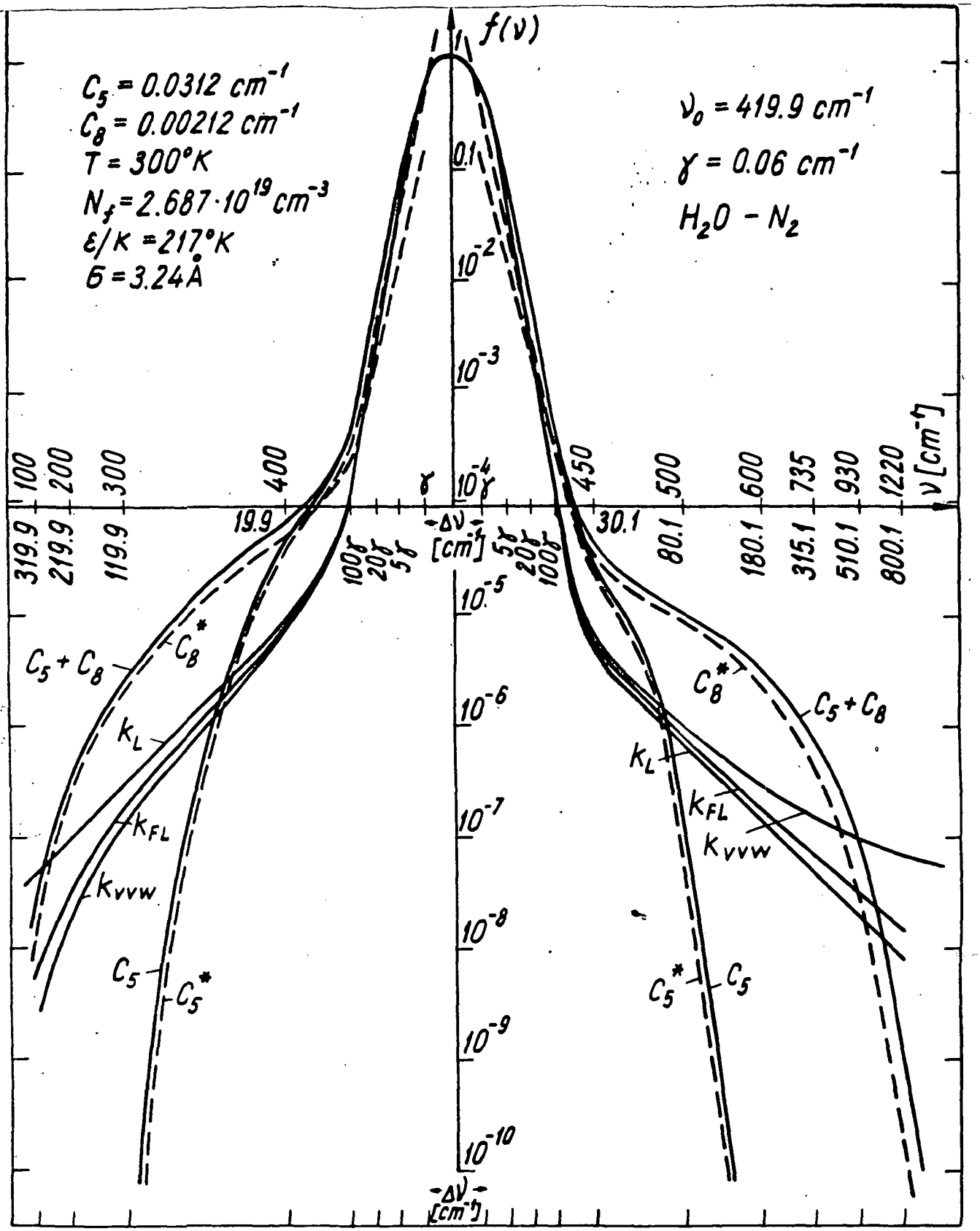

Figure 2. Line form factor f(ν) vs. frequency ν and frequency shift Δν for various contours: solid curves, form factor according to Lorentz contour (k_L) "complete" Lorentz contour and contour according to kinetic equation (k_{FL}), "Van Vleck-Wiesskopf contour" (k_{VVW}), generalized line contour with varied modeling of resonance frequency shift (C_5, $C_5 + C_8$); dashed curves (C_5^X and C_8^X), form factor according to line wing formulas [1] with varied modeling of $\Delta(R)$.

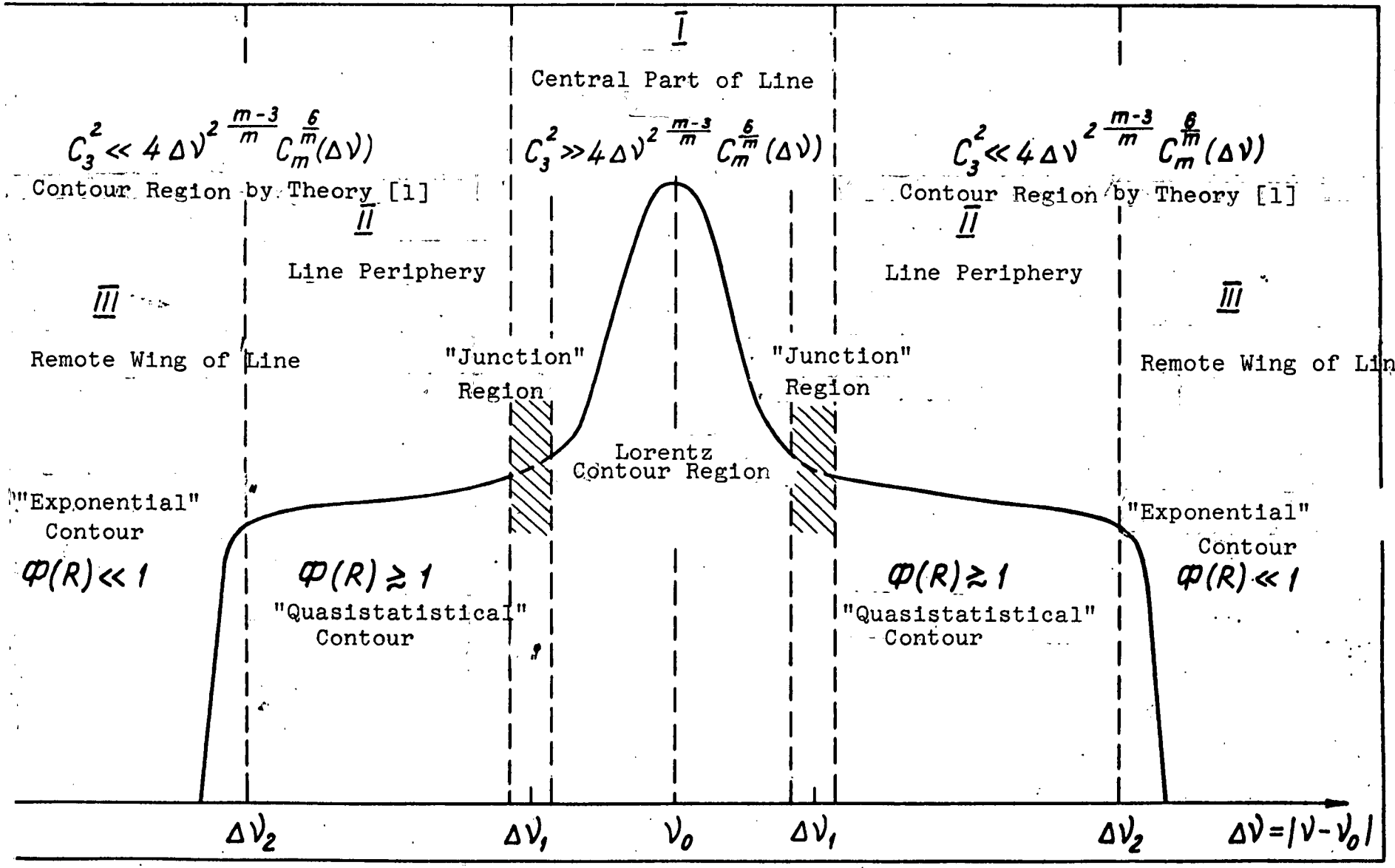

Figure 3. Diagram of line wing breakdown into different frequency shift regions ($\Delta\nu$): Each Region corresponds to its own type of contour in accordance with condition (28) and behavior of function $\Phi(R)$ (21).

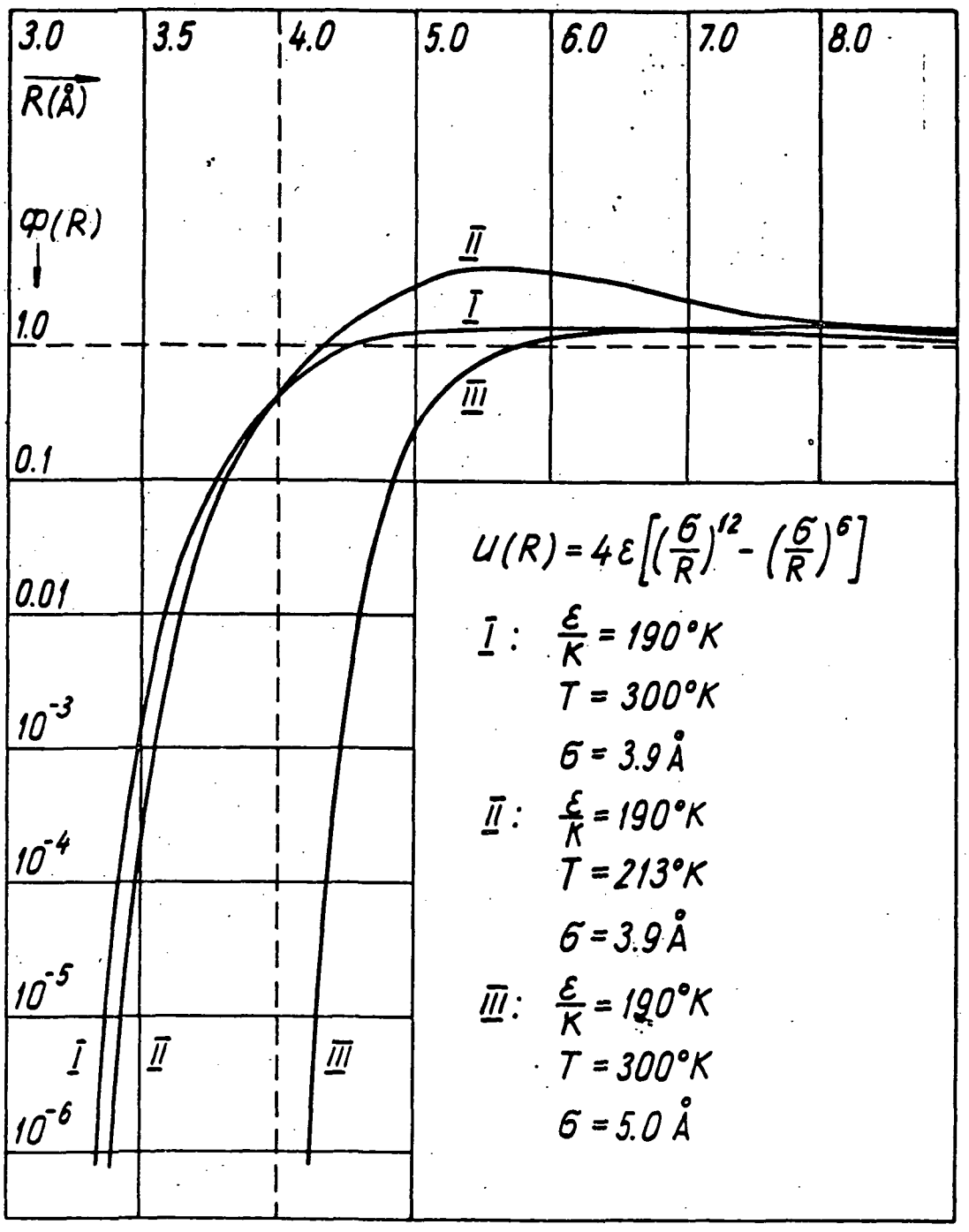

Figure 4. Function Φ(R)(21) vs. intermolecular distance R with various classical interaction potential parameters and temperatures.

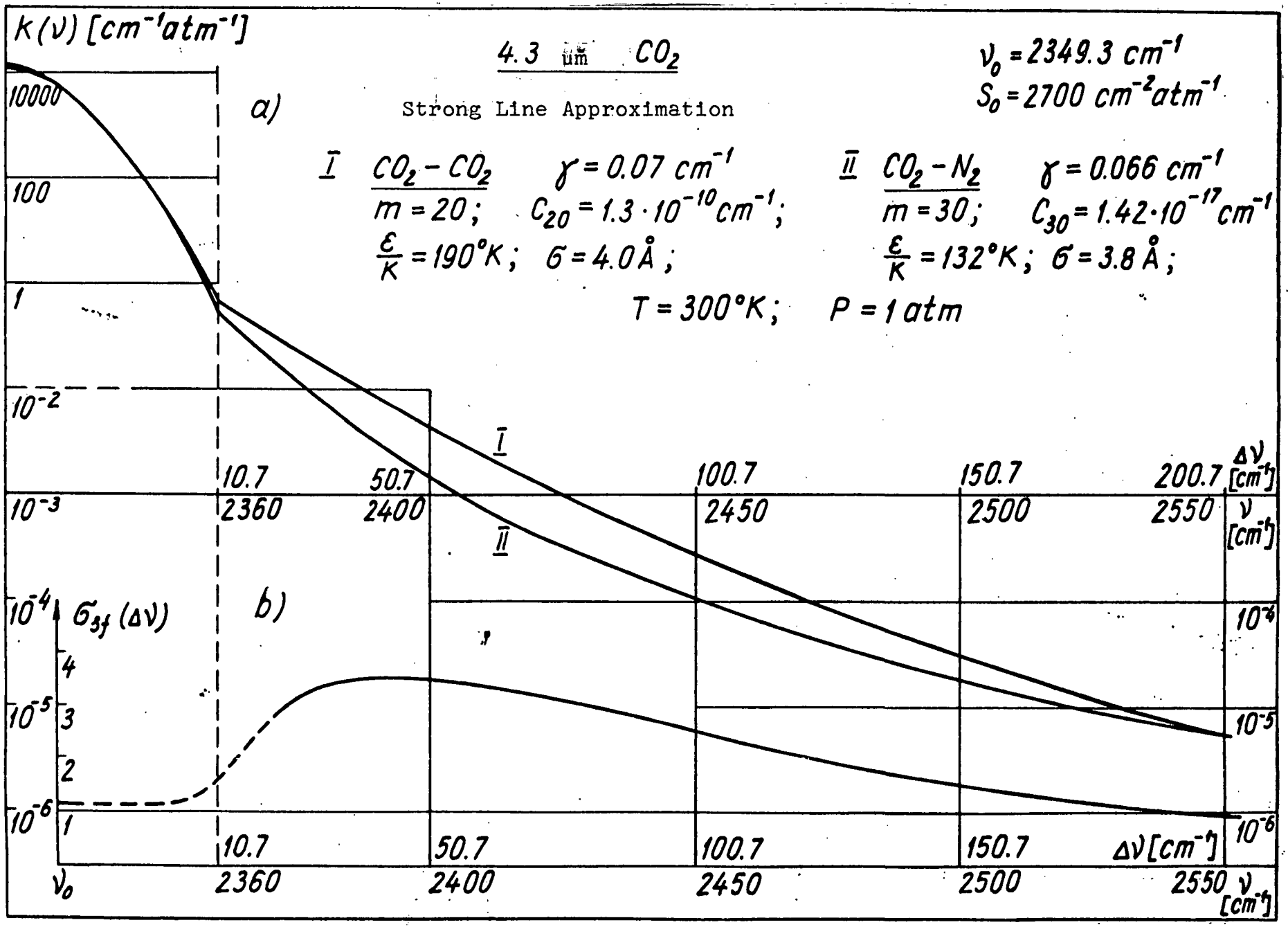

Figure 5. (a) absorption k(ν) and (b) self-broadening coefficient σ_{sf} (Δν) vs. frequency ν and frequency shift Δν; dashed line designates change of scale on abscissa.

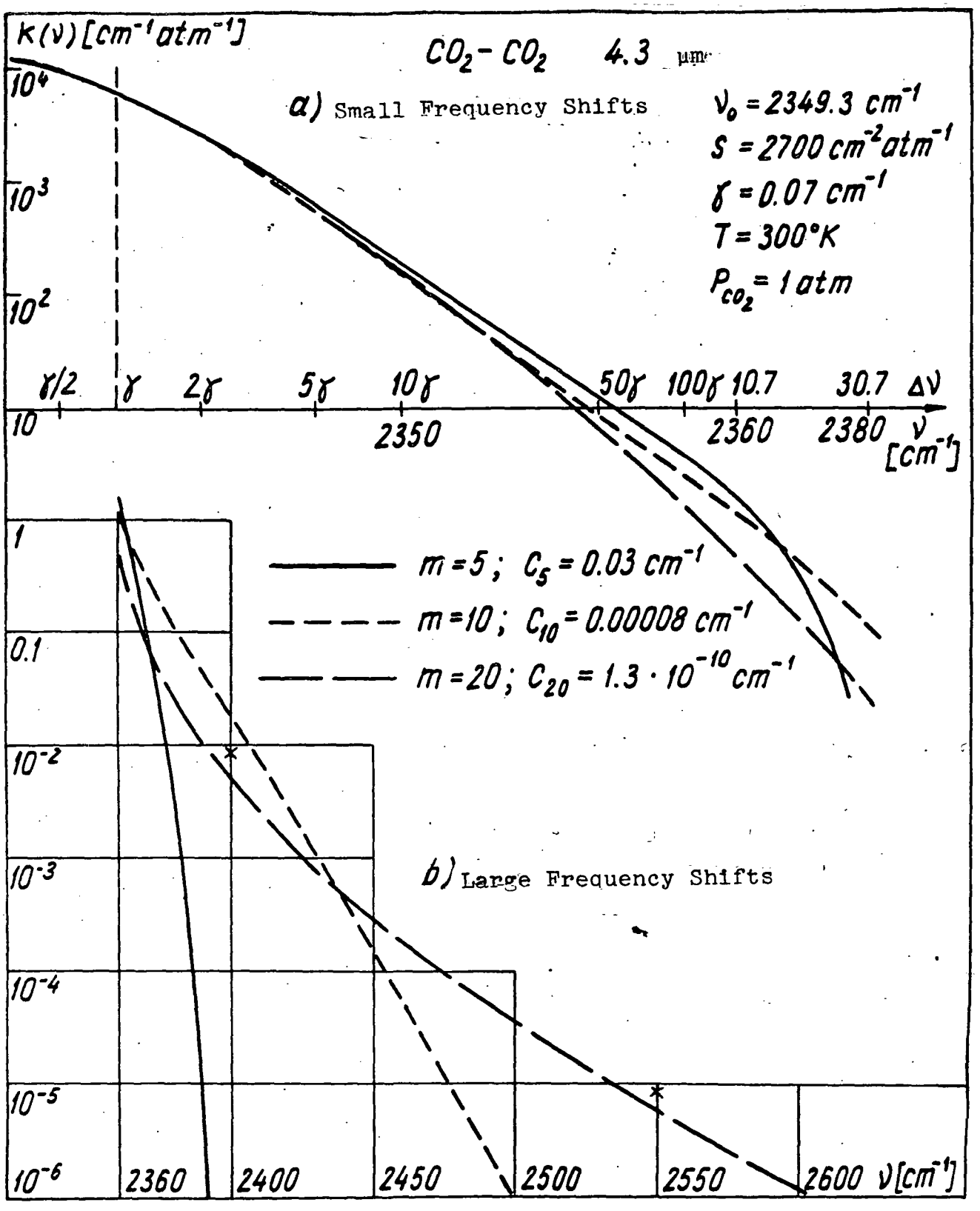

Figure 6. Absorption coefficient k(ν) vs. frequency ν and frequency shift Δν in "strong line approximation" for 4.3 μm band (self-broadening case): curves correspond to different multipole approximations for resonance frequency shift; experimenta data of [3] plotted in part (b) of figure for 2400 cm^{-1} and 2550 cm^{-1} on abscissa beyond dashed line in part (a), scale changed.

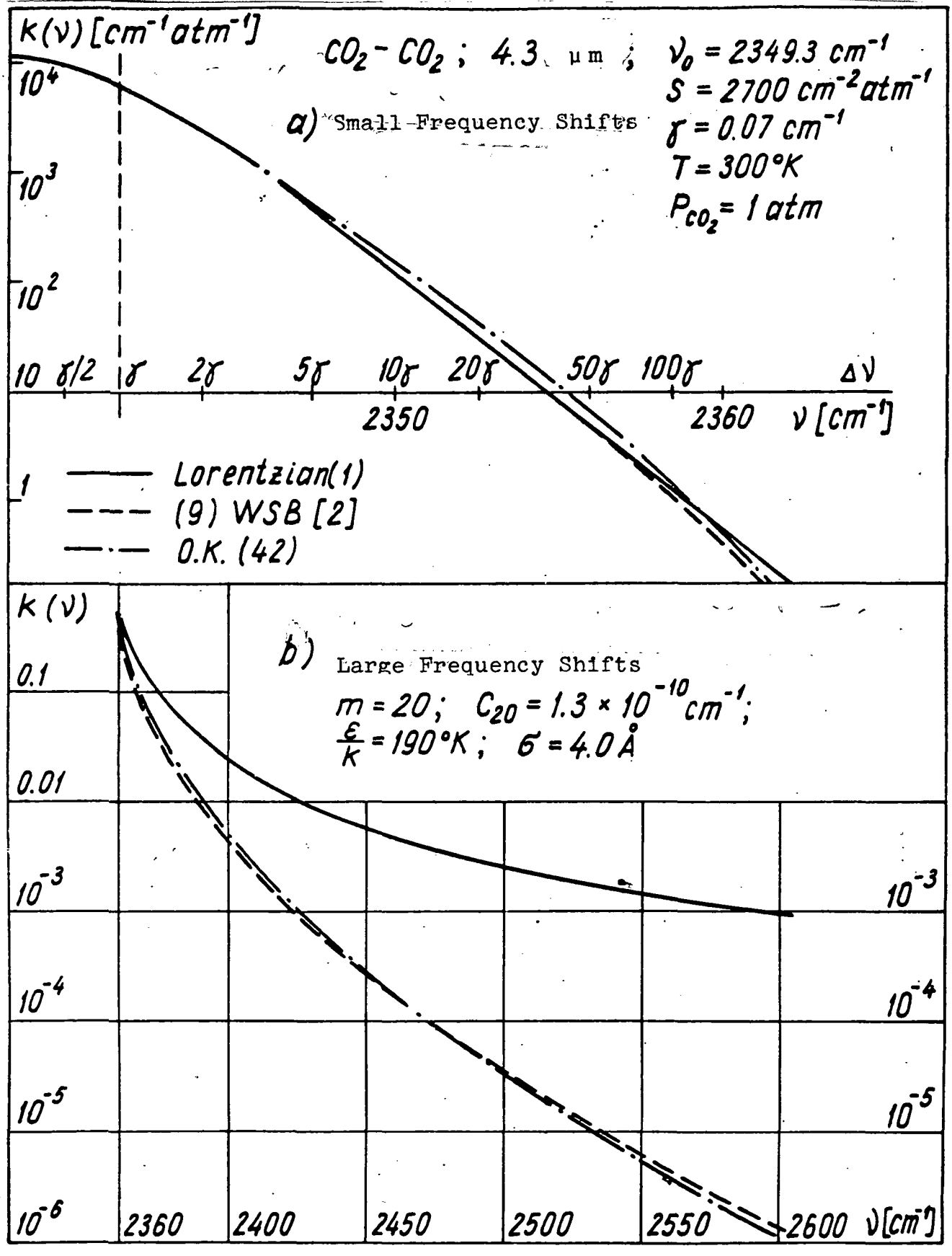

Figure 7. Absorption coefficient k(ν) vs. frequency ν and frequency shift Δν in "strong line approximation" for 4.3 μm CO_2 band with various line contours (self-broadening case): vertical dashed line distinguishes transition to continuous change of scale on abscissa in part (a) of figure.

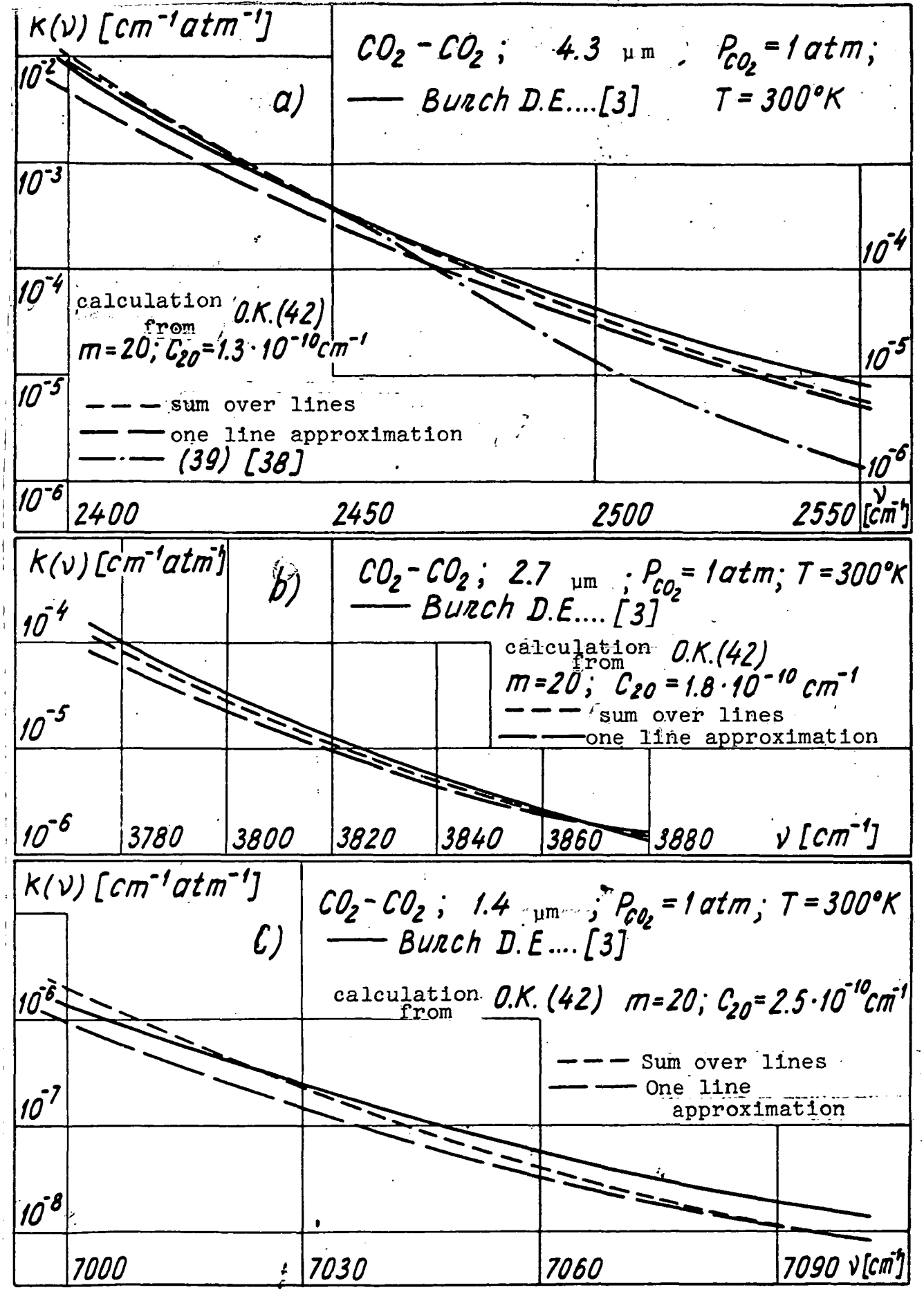

Figure 8. Absorption coefficient k(ν) vs. frequency ν in nigh frequency wings of 4.3 μm, 2.7 μm, 1.4 μm CO_2 bands (self-broadening case).

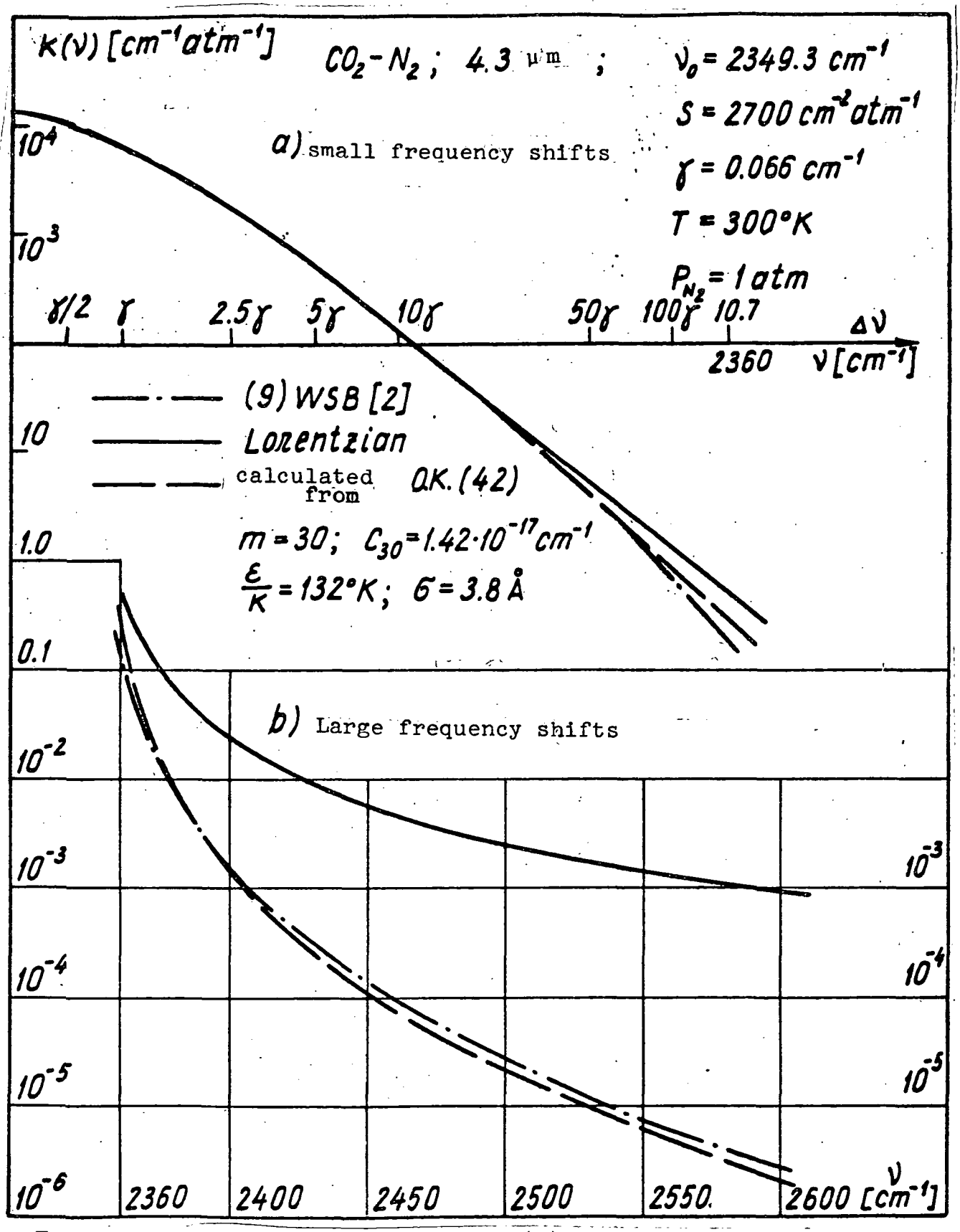

Figure 9. Absorption coefficient k(ν) vs. frequency ν and frequency shift Δν in "strong line approximation" for 4.3 μm CO_2 band with various line contours (nitrogen broadening case).

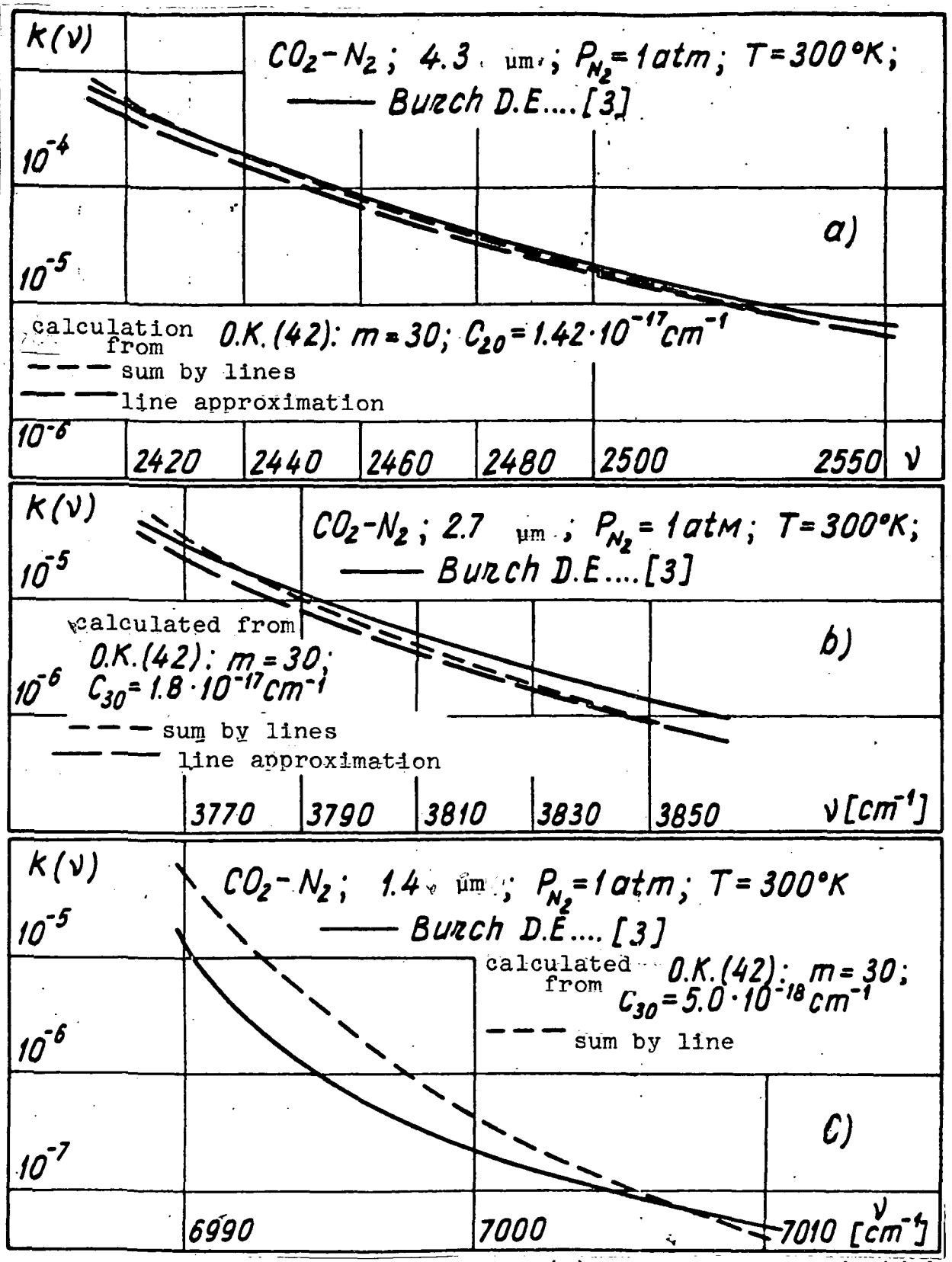

Figure 10. Absorption coefficient k(ν) vs. frequency ν in high frequency wings of 4.3 μm, 2.7 μm, 1.4 μm CO_2 bands (nitrogen broadening case).

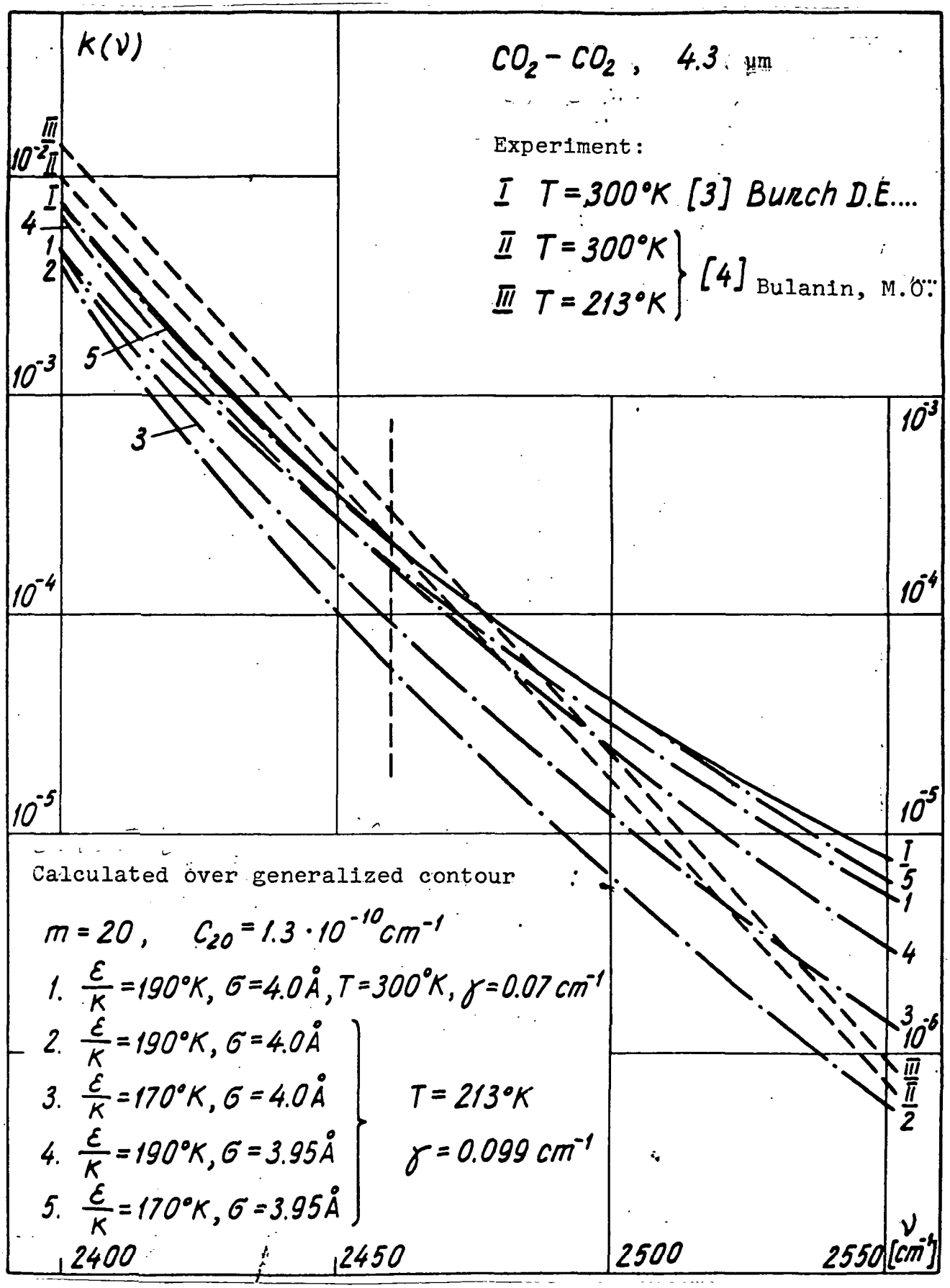

Figure 11. Absorption coefficient k(ν) vs. frequency ν beyond edge of high frequency wing of 4.3 μm CO_2 band at various temperatures from experimental data and from generalized contour with variations of function U(R) (self-broadening case).

Appendix 2. Tables

Table 1. Line form factor $f(\nu)$ vs. frequency ν at frequency shift $\Delta\nu$ for various contours (for Fig. 1.).

Table 2. Line form factor $f(\nu)$ vs. frequency ν at frequency shift $\Delta\nu$ for various contours (for Fig. 2).

Table 3. Function $\Phi(R)$ (21) vs. intermolecular distance R with various classical interaction potential parameters and temperatures (for Fig. 4).

Table 4. Absorption coefficient $k(\nu)$ and self-broadening coefficient $\sigma_{sf}(\Delta\nu)$ vs. frequency ν and frequency shift $\Delta\nu$ (for Fig. 5).

Table 5. Absorption coefficient $k(\nu)$ vs. frequency ν and frequency shift $\Delta\nu$ in "strong line approximation" for 4.3 μm band (self-broadening case) (for Fig. 6) with various multipole interactions.

Table 6. Absorption coefficient $k(\nu)$ vs. frequency ν and frequency shift $\Delta\nu$ in "strong line approximation" for 4.3 μm CO_2 band with various line contours (self-broadening case) (for Fig. 7).

Table 7. Absorption coefficient $k(\nu)$ vs. frequency ν in high frequency wings of 4.3 μm, 2.7 μm, 1.4 μm CO_2 bands (self-broadening case)(for Fig. 8).

Table 8. Absorption coefficient $k(\nu)$ vs. frequency ν and frequency shift $\Delta\nu$ in "strong line approximation" for 4.3 μm CO_2 band with various line contours (nitrogen broading case) (for Fig. 9).

Table 9. Absorption coefficient $k(\nu)$ vs. frequency ν in high frequency wings of 4.3 μm, 2.7 μm, 1.4 μm CO_2 bands (nitrogen broadening case) (for Fig. 10).

Table 10. Absorption coefficient $k(\nu)$ vs. frequency ν beyond edge of high frequency wing of 4.3 μm CO_2 band at various temperatures from experimental data and from generalized contour with variations of function U(R) (self-broadening case) (for Fig. 11).

Table 1 (data for Fig. 1)

Line form factor $f(\nu)$ vs. frequency ν and frequency shift $\Delta\nu$ for various contours.

Calculation parameters: H_2O-N_2

$\nu_0 = 18.58\,cm^{-1}$; $\gamma = 0.111\,cm^{-1}$; $C_4 = 0.02\,cm^{-1}$; $C_5 = 0.0312\,cm^{-1}$; $C_8 = 0.00212\,cm^{-1}$; $N_{N_2} = 2.687 \cdot 10^{19}\,cm^3$; $T = 300^\circ K$; $\varepsilon/K = 217^\circ K$; $\sigma = 3.24$ Å

ν cm^{-1}	$\Delta\nu$ cm^{-1}	line form factor $f(\nu)$ (1) k_L	(2) k_{FL}	(5) k_{VVW}	(42) OK. C_4	(42) OK. C_4+C_5	(42) OK. C_8+C_8
0.5	18.02	3.76'-5	1.05'-7	5.20'-8	1.43'-9	1.73'-7	1.96'-7
2.0	16.58	4.47'-5	1.70'-6	8.57'-7	6.07'-8	2.84'-6	3.20'-6
5.0	13.58	6.69'-5	1.19'-5	6.43'-6	2.34'-6	2.03'-5	2.27'-5
10.0	8.58	1.68'-4	8.20'-5	5.30'-5	5.96'-5	1.40'-4	1.50'-4
13.6	4.98	4.96'-4	3.55'-4	2.72'-4	3.43'-4	5.83'-4	6.01'-4
15.5	3.08	1.30'-3	1.07'-3	0.91'-3	1.07'-3	1.64'-3	1.66'-3
17.47	10 γ	9.90'-3	9,31'-3	8.77'-3	9.01'-3	1.20'-2	1.19'-2
18.025	5 γ	3.85'-2	3.73'-2	3,63'-2	3.54'-2	4.29'-2	4.29'-2
18.358	2 γ	2.00'-1	1.98'-1	1.95'-1	1.84'-1	2.03'-1	2.06'-1
18.469	γ	5.00'-1	4.97'-1	4.94'-1	4.62'-1	4.80'-1	4.92'-1
18.691	γ	5.00'-1	5.03'-1	5.06'-1	4.73'-1	4.91'-1	5.04'-1
18.802	2 γ	2.00'-1	2.02'-1	2.05'-1	1.93'-1	2.13'-1	2.16'-1
19.135	5 γ	3.85'-2	3.97'-2	4.09'-2	3.97'-2	4.82'-2	4.82'-2
19.69	10 γ	9.90'-3	1.05'-2	1.11'-2	1.14'-2	1.51'-2	1.50'-2
22.4	3.82	8.45'-4	1.02'-3	1.24'-3	1.49'-3	2.36'-3	2.40'-3
34.2	15.62	5.05'-5	8.46'-5	1.86'-4	3.18'-5	5.48'-4	6.59'-4
50.0	31.42	1.24'-5	2.62'-5	1.09'-4	4.60'-18	3.12'-4	5.30'-4
100.0	81.42	1.80'-6	5.26'-6	7.92'-5	0	1.15'-5	5.16'-4
200.0	181.42	3.70'-7	1.25'-6	7.31'-5	0	1.05'-17	4.03'-4
500.0	481.42	5.30'-8	1.97'-7	7.17'-5	0	0	3.60'-5

Table 2 (data for Fig. 2)

Line form factor $f(\nu)$ vs. frequency ν and frequency shift $\Delta\nu$ for various contours.

Calculation parameters: $\nu_0 = 419.9\,cm^{-1}$; $\gamma = 0.06\,cm^{-1}$; $C_5 = 0.0312\,cm^{-1}$;

$H_2O - N_2$ $C_8 = 0.00212\,cm^{-1}$; $N_{N_2} = 2.687 \cdot 10^{19}\,cm^{-3}$;

$T = 300^0K$; $\frac{\varepsilon}{k} = 217^0K$; $\sigma = 3.24$ Å.

ν cm^{-1}	$\Delta\nu$ cm^{-1}	line form factor $f(\nu)$ (1) k_L	(2) k_{FL}	(3) k_{VVW}	(4-2) $OK.\ C_5$	[4] C_5^*	(4-2) $OK.\ C_5 + C_8$	[4] C_8^*
100.0	319.9	4.85'-8	5.20'-9	2.75'-9	0	0	3.37'-8	1.64'-8
200.0	219.9	8.40'-8	3.08'-8	1.91'-8	0	0	3.58'-7	2.46'-7
300.0	119.9	2.58'-7	1.74'-7	1.31'-7	3.04-12	2.36-13	2.46'-6	1.87'-6
400.0	19.9	9.08'-6	8.70'-6	8.28'-6	4.76'-5	4.10'-5	5.72'-5	4.21'-5
413.9	6.0	1.00'-4	9.88'-5	9.74'-5	3.48'-4	3.00'-4	3.60'-4	2.18'-4
418.7	20γ	2.50'-3	2.49'-3	2.48'-3	4.94-3	3.50'-3	4.86'-3	1.95'-3
419.6	5γ	3.85'-2	3.84'-2	3.84'-2	5.29'-2	3.22'-2	5.21'-2	1.27'-2
419.84	γ	5.00'-1	5.00'-1	5.00'-1	5.30'-1	4.25'-1	5.28'-1	1.14'-1
419.87	$\gamma/2$	8.00'-1	8.00'-1	8.00'-1	8.04'-1	1.29'-0	8.03-1	2.97'-1
419.93	$\gamma/2$	8.00'-1	8.00'-1	8.00'-1	8.04'-1	1.29'-0	8.03'-1	2.97'-1
419.96	γ	5.00'-1	5.00'-1	5.00'-1	5.30'-1	4.25'-1	5.28'-1	1.14'-1
420.20	5γ	3.85'-2	3.85'-2	3.85-2	5.30'-2	3.23'-2	5.22'-2	1.27'-2
421.1	20γ	2.50'-3	2.50'-3	2.50'-3	4.98'-3	3.53'-3	4.89'-3	1.95'-3
425.9	6.0	1.00'-4	1.02'-4	1.03'-4	3.62'-4	3.11'-4	3.73'-4	2.18'-4
450	30.1	3.98'-6	4.26'-6	4.58'-6	2.38'-5	1.99'-5	3.64'-5	2.76'-5
500	80.1	5.65'-7	6.67'-7	8.01'-7	9.35'-8	3.34'-8	9.61'-6	8.04'-6
600	180.1	1.14'-7	1.54'-7	2,34'-7	1.10-23	0	2.68'-6	1.90'-6
735	315.1	3.90'-8	5.86'-8	1.20'-7	0	0	6.63'-7	3.43'-7
930	510.1	1.58'-8	2.63'-8	7.77'-8	0	0	6.91'-8	2.58'-8
1220	800.1	6.96'-9	1.23'-8	5.87'-8	0	0	9.96'-10	2.19'-10

Table 3 (data for Fig. 4)

Function $\varphi(R)_{(2I)}$ vs. intermolecular distance R with various classical interaction potential parameters and temperatures.

$\varepsilon/k = 190^\circ K$					
$T=300^\circ K, \sigma=3.9\,A^\circ$		$T=213^\circ K, \sigma=3.9\,A^\circ$		$T=300^\circ K, \sigma=5.0\,A^\circ$	
R A°	$\varphi(R)$	R A°	$\varphi(R)$	R A°	$\varphi(R)$
3.32	I.80'-6	3.39	I.64'-6	4.26	I.80'-6
3.44	2.84'-4	3.54	8.80'-4	4.4I	2.84'-4
3.60	I.26'-2	3.72	3.92'-2	4.62	I.26'-2
3.675	3.85'-2	3.8I	I.04'-I	4.7I	3.85'-2
3.89	2.48'-I	3.92	2.52'-I	4.99	2.48'-I
4.00	3.99'-I	4.07	5.40'-I	5.I3	3.99'-I
4.28	7.59'-I	4.33	9.8' -I	5.49	7.59'-I
4.64	I.0I4"-0	5.34	I.32'-0	5.95	I.0I4'-0
6.40	I.083'-0	7.46	I.I3'-0	8.2I	I.083'-0
7.835	I.049'-0	8.92	I.08'-0	I0.04	I.049'-0

Table 4 (data for Fig. 5)

Absorption coefficient $k(\nu)$ and self-broadening coefficient $\delta_{sf}(\Delta\nu)$ vs. frequency ν and frequency shift $\Delta\nu$

Calculation parameters: "Strong line approximation"
$\nu_0 = 2349.3$ см$^{-1}$; $S = 2700$ см$^{-2}$атм$^{-1}$; $T = 300^\circ$K.
$P = 1$ атм.

Размерность: $[\nu]=[\Delta\nu]=$ см$^{-1}$; $[k]=$ см$^{-1}$атм$^{-1}$.

		CO_2-N_2			CO_2-CO_2			
		$\gamma_1=0.066$ см$^{-1}$; $\frac{\varepsilon}{k}=132^\circ$K; $C_{30}=1.42\cdot10^{-17}$ см$^{-1}$; $\delta=3.8$ A°			$\gamma_2=0.07$ см$^{-1}$; $\frac{\varepsilon}{k}=190^\circ$K; $C_{20}=1.3\cdot10^{-10}$ см$^{-1}$; $\delta=4$ A°			
ν	$\Delta\nu$	(1) k_L	(2) ОК. $m=30$	$\frac{k_{ОК}}{k_L}$	(1) k_L	(2) ОК. $m=20$	$\frac{k_{ОК}}{k_L}$	$\delta_{sf}(\Delta\nu)$
2349.333	$0.5\gamma_1$	1.04'+4	1.04'+4	1.0006	-	-	-	
2349.34	$0.6\gamma_2$	-	-	-	9.26 +3	9.27 +3	1.002	
2349.46	$2.3\gamma_2$	-	-	-	1.97 +3	2.02 +3	1.021	
2349.465	$2.5\gamma_1$	1.80'+3	1.82'+3	1.013	-	-	-	
2349.63	$5\gamma_1$	5.01'+2	5.15'+2	1.029	-	-	-	
2349.70	$5.7\gamma_2$	-	-	-	3.64'+2	4.21'+2	1.155	
2360	10.7	4.95'-1	3.07'-1	0.620	5.25'-1	4.75'-1	0.905	1.55
2380	30.7	6.02'-2	7.63'-3	0.127	6.39'-2	2.57'-2	0.402	3.97
2400	50,7	2.21'-2	1.34'-3	0.061	2.34'-2	4.70'-3	0.201	3.51
2420	70.7	1.13'-2	4.09'-4	0.036	1.20'-2	1.31'-3	0.109	3.20
2440	90.7	6.89'-3	1.62'-4	0.024	7.31'-3	4.50'-4	0.062	2.78
2450	100.7	5.59'-3	1.05'-4	0.019	5.93'-3	2.66'-4	0.045	2.53
2460	110.7	4.63'-3	7.22'-5	0.016	4.91'-3	1.67'-4	0.034	2.31
2480	130.7	3.32'-3	3.71'-5	0.011	3.52'-3	7.04'-5	0.020	1.90
2500	150.7	2.50'-3	2.06'-5	0.008	2.65'-3	3.17'-5	0.012	1.54

Table 5 (data for Fig. 6)

Absorption coefficient $k(\nu)$ vs. frequency ν and frequency shift $\Delta\nu$ in "strong line approximation" for 4.3 μm band (self-broadening case) with various multipole interactions.

Calculation parameters: "Strong line approximation"

$\nu_0 = 2349.3\,cm^{-1}$ $S = 2700\ cm^{-2}\ atm^{-1}$;
$\gamma = 0,07\ cm^{-1}$; $T = 300^0K$; $P = 1\ atm$.

ν cm^{-1}	(42) C_5 $0,03\,cm^{-1}$	$k(\nu)(cm^{-1}\ atm^{-1})$ C_{10} $8.0'-5\,cm^{-1}$	C_{20} $13'-10\,cm^{-1}$
2349.34	9.23'+3	9.40'+3	9.27'+3
2349.38	5.57'+3	5.53'+3	5.36'+3
2349.46	2.23'+3	2.I4'+3	2.02'+3
2349.7	4.96'+2	4.34'+2	4.2I'+2
2350.I	I.50'+2	I.I6'+2	I.3I'+2
2353.3	I.00'+I	6.33'+0	6.3I'+0
2357.3	2.98'+0	I.98'+0	I.02'+0
2360	I.6I'+0	I.I3'+0	4.75'-I
2380	3.05'-3	I.05'-I	2.57'-2
2400	7.73'-I0	I.62'-2	4.70'-3
24I0	3.57'-I5	6.53'-3	2.4I'-3
2420	4.40'- 22	2.62'-3	I.3I'-3
2430	0	I.03'-3	7.54'-4
2440	0	3.86'-4	4.50'-4
2450	0	I.47'-4	2.60'-4
2460	0	5.50'-5	I.67'- 4
2480	0	7.32'-6	7.04'-5
2500	0	9.I3'-7	3.I7'-5
2550	0	3.66'-9	5.3I'-6
2600	0	I.08'-II	I.09'-6

Table 6 (data for Fig. 7)

Absorption coefficient $k(\nu)$ vs. frequency ν and frequency shift $\Delta\nu$ in "strong line approximation for 4.3 μm CO_2 band with various line contours (self-broadening case).

Calculation Parameters: "Strong line approximation"

$\nu_0 = 2349.3 cm^{-1}$; $S = 2700 cm^{-2} atm^{-1}$; $\gamma = 0.07 cm^{-1}$

$C_{20} = 1.3 \cdot 10 cm^{-1}$; $T = 300^0 K$; $P = 1$ atm.

$\varepsilon/k = 190^0 K$; $\sigma = 4$ Å

Dimensions: $[\nu] \equiv [\Delta\nu] = cm^{-1}$; $[k] = cm^{-1} atm^{-1}$.

ν	$\Delta\nu$	(1) k_L	WSB [2] k_{WSB}	$\frac{k_{WSB}}{k_L}$	(42) k_{OK}	$\frac{k_{OK}}{k_L}$
2349.335	$\gamma/2$	9.82'+3	9.82'+3	1.000	9.84'+3	1.002
2349.370	γ	6.14'+3	6.14'+3	1.000	6.17'+3	1.005
2349.440	2γ	2.46'+3	2.45'+3	1.000	2.50'+3	100
2349.650	5γ	4.72'+2	4.72'+2	10000	5.33'+2	1.018
2350.0	10γ	1.22'+2	1.22'+2	1.000	1.63'+2	1.340
2350.7	20γ	3.06'+1	3.06'+1	1.000	5.51'+1	1.801
2352.8	50γ	4.91'+0	4.91'+0	1.000	8.81'+0	1.794
2356.3	100γ	1.23'+0	1.07'+0	0.870	1.45'+0	1.179
2360.0	10.7	5.25'-1	3.81'-1	0.725	4.75'-1	0.905
2380	30.7	6.38'-2	2.18'-2	0.342	2.57'-2	0.403
2400	50.7	2.34'-2	4.26'-3	0.182	4.70'-3	0.201
2420	70.7	1.20'-2	1.24'-3	0.103	1.31'-3	0.109
2430	80.7	9.23'-3	7.22'-4	7.82'-2	7.54'-4	8.2'-2
2440	90.7	7.31'-3	4.38'-4	5.99'-2	4.50'-4	6.2'-2
2450	100.7	5.93'-3	2.74'-4	4.62'-2	2.66'-4	4.5'-2
2460	110.7	4.91'-3	1.76'-4	3.58'-2	1.67'-4	3.4'-2
2480	130.7	3.52'-3	7.67'-5	2.18'-2	7.04'-5	2.0'-2
2500	150.7	2.65'-3	3.58'-5	1.35'-2	3.17'-5	1.2'-2

Table 7 (data for Fig. 8)
Absorption coefficient $k(\nu)$ vs. frequency ν in high frequency wings of 4.3 μm, 2.7 μm, 1.4 μm CO_2 bands (self-broadening case)

Calculation parameters: $\varepsilon/k = 190^{\circ}K$; $\sigma = 4.0$ A; $\gamma = 0.07\ cm^{-1}$; $T = 300^{\circ}K$; $P = 1$ atm.

Dimensions: $[\nu] \equiv [\Delta\nu] = cm^{-1}$; $[k(\nu)] = cm^{-1}atm^{-1}$

a. 4.3 μm: $m = 20$, $C_{20} = 1.3' - 10\ cm^{-1}$;
b. 2.7 μm: $m = 20$, $C_{20} = 1.8' - 10\ cm^{-1}$;
c. 1.4 μm: $m = 20$, $C_{20} = 2.5' - 10\ cm^{-1}$;

	ν	[3] experiment	(42) Gen. contour Σ	(42) Gen. contour ПСЛ	$k_{\Sigma}/k_{[3]}$	[2] WSB	[38] (39)
	2400	8.0'-3	I0.5'-3	4.7'-3	+ 3I%	4.5'-3	8.4'-3
	2420	2.I'-3	208'-3	I.3'-3	- I%	I.3'-3	I.9'-3
a)	2440	7.5'-4		4.5'-4		4.5'-4	6.6'-4
	2460	2.0'-4	2.I7'-4	I,7'-4	+8%	I.8'-4	I.8'-4
	2500,	4.I'- 5	3.72'-5	3.2'-5	-9%	3.7'-5	I.2'-5
	2550	8.0'-6	5.9'-6	5.3'-6	-24%	6.6'-6	I.4'-6
	3780	I.0'-4	0.82'-4	0.60'-4	-I8%		
	3800	3.4'-5	2.75'-5	2.3'-5	-I9%		
b)	3820	I.4'-5	I,2'-5	9.8'-6	-2I%		
	3850	3.5'-6	3.48'-6	3.I'-6	- I%		
	3870	I.6'-6	I.7'-6	I.6'-6	+6%		
	7000	I.4'-6	2.I'-6	0.98'-6	+50%		
c)	7030	2.4'-7	I.66'-7	I.4'-7	-3I%		
	7060	8.0'-8	4.0'-8	3.7'- 8	-50%		
	7I00	I.4 '-8	0.97'-8	0.97'-8	-3I%		

Table 8 (data for Fig. 9)

Absorption coefficient k(ν) vs. frequency ν and frequency shift Δν in "strong line approximation" for 4.3 μm CO_2 band with various line contours (nitrogen broadening case)

Parameters: calculation in "strong line approximation"

$\nu_0 = 2349.3 см^{-1}$; $S = 2700\ см^{-1}{}_{атм}{}^{-1}$

$\gamma = 0.066\ см^{-1}$; $C_{30} = 1.42'-17 см^{-1}$; $T = 300^{\circ}K$

$N_{N_2} = 2.687 \cdot 10^{19} см^3$

Dimensions: $[\nu] \equiv [\Delta\nu] = см^{-1}$; $[k] = см^{-1}{}_{атм}{}^{-1}$.

ν	$\Delta\nu$	(1) k_L	WSB [2] k_{WSB}	$\frac{k_{WSB}}{k_L}$	(42) k_{OK}	$\frac{k_{OK}}{k_L}$
2349.333	$\gamma/2$	1.04'+4	1.04'+4	1.000	1.04'+4	1.000
2349.465	2.5γ	1.80'+3	1.80'+3	1.000	1.82'+3	1.013
2349.63	5γ	5.01'+2	5.01'+2	1.000	5.15'+2	1.029
2360.0	10.7	4.95'-1	1.78'-1	0.359	3.07'-1	0.620
2380.0	30.7	6.02'-2	7.77'-3	0.129	7.63'-3	0.127
2400	50.7	2.21'-2	1.53'-3	6.93'-2	1.34'-3	6.06'-2
2420	70.7	1.13'-2	4.83'-4	4.27'-2	4.09'-4	3.62'-2
2440	90.7	6.88'-3	1.95'-4	2.83'-2	1.62'-4	2.35'-2
2450	100.7	5.59'-3	1.31'-4	2,35'-2	1.05'-4	1.88'-2
2460	110.7	4.64'-3	9.14'-5	1.97'-2	7.22'-5	1.56'-2
2480	130.7	3.35'-3	4.79'-5	1.43'-2	3.71'-5	1.11'-2
2500	150.7	2.49'-3	2.64'-5	1.06'-2	2.06'-5	8.3'-3
2550	200.7	1.38'-3	7.53'-6	5.46'-3	5.94'-6	4.3'-3
2600	250.7	9.45'-4	2.90'-6	3.07'-3	2.13'-6	2.3 -3

Table 9 (data for Fig. 10)

Absorption coefficient k(ν) vs. frequency ν in high frequency wings of 4.3 μm, 2.7 μm, 1.4 μm CO_2 bands (nitrogen broadening case)

Calculation parameters: $\mathcal{E}/k = 132^{\circ}K$; $\sigma = 3.8$ Å; $\gamma = 0.066$ см$^{-1}$; $T = 300^{\circ}K$; $N_{N_2} = 2.687 \cdot 10^{19}$ см^3

Dimensions: $[\nu] = [\Delta\nu] =$ см$^{-1}$; $[k(\nu)] =$ см$^{-1}$ атм$^{-1}$.

a: 4,3 μм: $m = 30$, $C_{30} = 1.42'-17$ см$^{-1}$;

b: 2,7 μм: $m = 30$, $C_{30} = 1.8'-17$ см$^{-1}$;

c: 1,4 μм: $m = 30$, $C_{30} = 5.0'-18$ см$^{-1}$.

	ν	[3] эксперим.	(42) Обобщ. контур Σ	ПСЛ	$k_\Sigma / k_{[3]}$
	2420	5.1'-4	6.1'-4	4.1'-4	+20%
	2440	2.1'-4	2.0'-4	1,6'-4	-5%
a)	2460	1.0'-4	8.5'-5	7.2'-5	-15%
	2500	2.1'-5	2.2'-5	2.1'-5	+5
	2550	7.0'-6	6.1'-6	5.9'-6	-13%
	3770	3.1'-5	3.8'-5	2.3'-5	+23%
	3790	1.1'-5	1.0'-5	0.82'-5	-9%
b)	3810	5.6'-6	4.0'-6	3.6'-6	-29%
	3840	2.0'-6	1.3'-6	1.3'-6	-35%
	3860	1.1'-6	0.72'-6	0.71'-6	-35%
	6990	1.4'-5	5.4'-5	3.85'-7	3.9
c)	6994	1.3'-6	5.3'-6	1.56'-7	4.1
	7000	2.8'-7	4.4'-7	5.3'-8	1.6
	7004	1.1'-7	1.4'-7	3.5'-8	1.3
	7010	5.0'-8	4.1'-8	1.3'-8	0.82

Table 10 (data for Fig. 11)

Absorption coefficient k( ) vs. frequency beyond edge of high frequency wing of 4.3 m CO_2 band at various temperatures from experimental data and from generalized contour with variation of function U(R)(self-broadening case)

T	2400	2420	2440	2460	2500	2550	ν см$^{-1}$ / k(ν) см$^{-1}$ атм$^{-1}$
300°K	8.0 -3	2.I'-3	7.5'-4	2.0'-4	4.I'-5	8.0'-6	I [3]
	9.98'-3	2.8I'-3	7.93'-4	2.23'-4	I.77'-5	7.48'-7	II [4]
	4.7'-3	I.3'-3	4.5'-4	I.7'-4	3.2'-5	5.3'-6	I ОК (42)
	I4.3'-3	3:97 -3	I.IO'-3	3.04'-4	2.33'-5	9.38'-7	III [4]
	3.9'-3	7.6'-4	I.9'-4	5.6'-5	6.4'-6	6.0'-7	2 ОК (42)
2I3°K	4.6'-3	I.0'-3	2.8'-4	9.0'-5	I.2'-5	I.4'-6	3 ОК (42)
	6.7'-3	I.6'-3	4.7'-4	I.6'-4	2.4'-5	3.I'-6	4 ОК (42)
	7.6'-3	2.0'-3	6.5'-4	2.3'-4	4.I'-5	6.2'-6	5 ОК (42)

Generalized contour (42) calculation parameters:

"strong line approximation"

$m = 20$, $C_{20} = I.3 \cdot I0^{-I0}$ см$^{-I}$, $S = 2700$ см$^{-I}$атм$^{-I}$.

I ОК: $\gamma = 0.07$ см$^{-I}$; $\delta = 4.0$ Å; $\frac{\varepsilon}{k} = I90°K$; $\left(\frac{4\varepsilon}{kT} = 2.533\right)$.

2 ОК: $\gamma = 0.099$ см$^{-I}$; $\delta = 4,0$ Å; $\frac{\varepsilon}{k} = I90°K$; $\left(\frac{4\varepsilon}{kT} = 3.568\right)$.

3 ОК: $\gamma = 0.099$ см$^{-I}$; $\delta = 4.0$ Å; $\frac{\varepsilon}{k} = I70°K$; $\left(\frac{4\varepsilon}{kT} = 3.I92\right)$.

4 ОК: $\gamma = 0.099$ см$^{-I}$; $\delta = 3,95$ Å; $\frac{\varepsilon}{k} = I90°K$; $\left(\frac{4\varepsilon}{kT} = 3,568\right)$.

5 ОК: $\gamma = 0.099$ см$^{-I}$; $\delta = 3.95$ Å; $\frac{\varepsilon}{k} = I70°K$; $\left(\frac{4\varepsilon}{kT} = 3.I92\right)$.